acp-2016-212, "Near-surface and columnar measurements with a Micro Pulse Lidar of atmospheric pollen in Barcelona, Spain" by Sicard et al.

General comments from the authors: First of all, we want to thank the two referees of our paper for their time and revision of our work. There is a small change in the paper that we would like to indicate to the referees. We noticed that the pollen on the last day of the event, on March 31st, after 18UT is not removed from the atmosphere (as it was said in the initial submission). A look at Figure 2b evidences it: a strong volume depolarization ratio persists in the ABL after 18UT but not below 0.5 km where it comes down to values typical of the local, background aerosol in Barcelona. This non-depolarizing plume (< 0.5 km) is at the same time associated with high values of the backscatter coefficient (Figure 2a). We checked that the detection of the pollen plume height was erroneously found at the first range bin shown (near 0.16 km), and not near the top of the ABL as it should be. We corrected our script and ran it again for the last hours of March 31st. This re-run results in changes in h_{pol} and thus on all integrated parameters (AOD_{pol}, AOD_{pol} / AOD, $\overline{\delta^V}$ and $\overline{\delta^p}$) only for March 31st after 18UT. We updated the following figures: 5, 6 and 8 and all four tables, as well as the discussion related to March 31st. We insist that these little changes only affect the data from March 31st after 18 UT, and do not change anything to the conclusions of the paper.

Answers to Referee#1's comments

Overall comment:
The object of this paper is to analyze relationships between direct surface measurements of pollen and MPL data simultaneously observed, and also meteorological parameters including solar radiation for continuous pollination events in Barcelona.
The results are shown with many figures and tables, and discussed in detail on the phenomena. The results and discussion may be a little lengthy, e.g., as mentioned in the "P15, L20-L27". And the reviewer feels that the discussion is not satisfactory for readers because of less physical aspects of the relationships analyzed. For example, in section 5, they analyze and discuss the correlation with solar radiation. It is interesting that the correlation coefficients have been better when introducing the time-delay(t). They show better results of correlation coefficient, when t > 0 and t < 0 for different days. What is the physical meaning of the time-delay ? Also why do these values show positive and negative in neighboring two days?
Authors' reply: The idea behind the correlation analysis between the quantity of pollen dispersed in the atmosphere (parametrized by δV or δp) and the solar radiation was to see if the solar radiation, which during daytime creates convective ascendant motion of air masses, is a major factor of the vertical motion of pollen during daytime. This idea is also reinforced by the fact that during nighttime, i.e. without solar radiation, pollen is usually not detected in the PBL. The objective of the correlation analysis is well introduced in the first paragraph of Section 5.
The convective ascendant motion of air masses produced by the solar radiation reaching the ground is not instantaneous; it occurs with a determined time delay. The time delay introduced in the paper has the exact same meaning, and the question that we want to answer is: what is the time phase difference between the variations of the solar radiation and the ones of δV or δp? We find that the time delay is between 0 and -1, which indicates a time phase difference between 0 and 60 minutes. However on 28 march we have a surprising result: the δV or δp variations are ahead of time (t is positive) w.r.t. the solar radiation. The probable explanations for it, and expressed in the text, are that 28 March is one of the days with nocturnal pollen near-surface activity and with the highest wind speeds. On that particular day, the transport of pollen in the atmosphere was already occurring before (and without) the morning solar radiation.

Minor comments:
P2, L22: Do authors have any reasons of two kinds of character types, normal and italic when written in the following manner, e.g., "Ambrosia, Alnus, Artemisia, Betula, Corylus, Chenopodiaceae, Cupressaceae/Taxaceae" Such expression is also shown in other places. If these are common in this field, it is Okay, but if not, please change these into one type.
Authors' reply: This is related to botanical terms and the taxonomy nomenclature rules. The names of genus have to be written in italics or underlined, the names of families are written with the normal letter type. You can recognize the names of the families by the termination –aceae. It is necessary to maintain the types indicated in the submitted version in order to be correct from the botanical point of view of the paper.

P6, L23: "In the second half of March 2015 a strong anticyclone positioned in the Atlantic Ocean west of the Portuguese coast generated southeasterly winds in the northeastern part of the Iberian Peninsula." Is the wind direction correct? It must be northwesterly (not southeasterly) ?
Authors' reply: The referee is right. That was a mistake from our part. "southeasterly" has been replaced by "northwesterly" in the revised manuscript.

P7, L8 ant other places: The unit for counting the number concentration of pollen even for the daily mean should be "m-3", not "m-3 day-1". This expression is physically wrong. So in this case they should express in the following manner, the daily mean concentration of pollen is xxx "m-3". Also the unit of "m-3 h-1" is wrong, shown in other sentences and figures. These should be changed.

Authors' reply: Initially "day-1" and "h-1" were added in order to indicate clearly if we were talking of daily or hourly averages. However we agree with the referee that it makes the units of concentration not fully correct, since the concentration numbers are not assessed by dividing by a unit of time (day or hour). So all pollen concentrations have been expressed in m-3 in the revised manuscript.

P8, L28: Is "Figure 3b" correct? It looks like "Figure 5."

Authors' reply: Figure 3b is correct. In Fig. 3b, as mentioned in the caption, the red and grey vertical lines indicate the time of the maximum pollen concentration and pollen optical depth, respectively, on each day.

P9, L21-L24: "Logically a strong release of … are gathered." It is a little hard to understand it. Please modify the sentence into much easier expression.

Authors' reply: This sentence and the previous one were replaced by the following: "As expected, every day the AOD_{pol} peak follows the total pollen concentration peak. Logically, in the case of pollen of local origin, not long-range transport, a peak of the amount of pollen in the atmosphere (parameterized by AOD_{pol}) can only happen if previously a strong release of pollen at the ground level (parametrized by the pollen concentration) has occurred.".

P13, L11-L13: "… is not from local origin." Please show and explain some evidences/reasons of "not from local origin."

Authors' reply: We have considerably modify the hypothesis related to the sudden removal of pollen on 31 March at 18h. The decrease of the pollen layer top height is associated with a strong increase of AOD, a strong increase of β^p in the first 0.5 km, a decrease of $\overline{\delta^V}$ and $\overline{\delta^p}$, an increase of RH but with no significant variation of the near-surface PM_{10} level. The characteristics of the layer below 0.5 km are thus not from sea salt (because we have low depolarization ratios), they are also not directly from the aerosols formed at ground level (PM levels are unchanged). We conclude to a water uptake (hygroscopic growth) of the already lofted particles and put it as a hypothesis in the text:

"Finally the sharp decrease of h_{pol} on 31 March at 18 UT is an indication of the sudden removal of the pollen from the ABL. This decrease of h_{pol} is associated with a strong increase of AOD due to high values of β^p (> 5 Mm^{-1} sr^{-1}) in the first 0.5 km (see ¡Error! No se encuentra el origen de la referencia.**), a decrease of $\overline{\delta^V}$ and $\overline{\delta^p}$, an increase of RH (see** ¡Error! No se encuentra el origen de la referencia.**b) but with no significant variation of the near-surface PM_{10} level. All in all these results suggest that the removal of the pollen from the ABL on 31 March at 18 UT may have been accompanied by a possible hygroscopic growth of lofted particles, probably from local origin, below 0.5 km."**

P14, L14: It is not so familiar with the following equation, "Pinus (0.09 <δV r -values < 0.70 and 0.25<δV r -values < 0.68),". Is it possible to change other expression for better understanding?

Authors' reply: "R-values" are correlation coefficients (their definition is given the first time they appear in the manuscript in Section 4) and "XX R-values" are the correlation coefficients measured between the parameter XX and another parameter. We have used this notation in order to synthetize the discussion as "XX R-values" is much shorter than "the correlation coefficients of XX". This notation also allows to treat "XX r-value" as a parameter and include it in equations like the one taken as example by the referee (0.09 < δ_V r -values < 0.70). In the

absence of a standard notation to express in a more concise way the “correlation coefficient of XX” the authors have decided to leave the notation “r-values” as is the manuscript.

P15, L20-L27: The reviewer supposes that the content of detailed cloud conditions is not necessarily needed in this context, because the cloud type such as medium or high might be not directly related with pollination events.
Authors’ reply: The most important for our analysis is that no low cloud was present during the pollination event (which could have made difficult the inversion of the lidar signals). The referee is right that the details on the medium and high clouds for the two cloudy days (29 and 30 March) are not necessary and they have been deleted in the revised manuscript. In turn the details have been kept for the three clear-sky days because we believe it is important to keep the detailed time of the presence of clouds (before 09:30UT on 27 March, before 10 and after 17UT on 28 March and after 17UT on 31 March) for the validation of the solar fluxes.

P17, L35: The sentence of “Otto et al.(2011) … ” may not be needed in this conclusion because the authors do not discuss on the radiative forcing in the main sections.
Authors’ reply: The effect of large pollen grains on the aerosol direct radiative forcing is only mentioned in the conclusions because it is a potential perspective that the authors would like to further investigate (in another paper). A small sentence “Large pollen grains may behave the same.” has been added at the end of the conclusions to get back to our topic: pollen (and not mineral dust).

Figure 1: The unit of “m-3day-1“ should be changed into “m-3”.
Authors’ reply: All concentration units have been changed.

Figure 2: The notation of decimal point should be unified, such as “0.005” from 0,005”. Also “km-1sr-1” should be unified into “Mm-1sr-1” because “Mm-1sr-1” is used in the text.
Authors’ reply: The dot (.) decimal separator has been used in the whole manuscript. The units of the backscatter coefficient have been unified as Mm-1 sr-1.

Figure 7: The colours of lines for 27th and 31st might be confused. These should be changed with other colours for discriminating clearly.
Authors’ reply: The authors have a different opinion and thought that the colours were rather well chosen. To satisfy the referee, we have kept the very different colours dark blue, brown, green and violet and changed the light blue by black. For homogeneity, the same colour change was applied to Figure 7.

Figure 8: The colour “red” is used for both of δP and time-delay. In order to understand these figures easily, the colours of δP and δV should be modified from “red” and “blue” into others.
Authors’ reply: δp is actually brown while the scatter plot with t=0 is effectively red. We have not applied the same line style as in Figure 4 (blue solid (δp) and dotted (δV) lines) because the symbols (solid circles) of Figure 8 would make difficult to differentiate them.

Answers to Referee#2's comments

Comment on "Near-surface and columnar measurements with a Micro Pulse Lidar of atmospheric pollen in Barcelona, Spain" by M. Sicard et al. More and more attentions have been paid on biological aerosols due to their significant impacts on environment and climate. The article presents an investigation of nearsurface and column characterization of atmospheric pollen in Barcelona, Spain, mainly by use of lidar measurements and sampling analysis. Moreover, impact of meteorological elements (e.g., RH, T and wind speed) and solar flux on atmospheric pollen load in the atmosphere was discussed in detail. The topic is of sufficient interest to the communities of study of atmospheric aerosol (especially bioaerosols), climate as well as human health. In general, I find this manuscript to be of interest for publication and appropriate for this journal. There are several suggestions for improvement listed below that should be considered by the authors and the editors before publication.

1. In fact, there is uncertainty during measurements of atmospheric pollen and spores. As introduced by the authors, pollen and spores was identified using a fluorescent microscope. However, the results should be affected by other fluorescent particles. It will be easier for readers to understand if the authors briefly introduce how to identify pollen and spores, obtain their concentration as well as discuss its uncertainty.
Authors'reply: Pollen and spores counts were performed by specialist technicians using light microscope, not fluorescent microscope. The explanation of pollen and spores identification has been rewritten in order to better describe the methodology used (Lines 26-34 of the initial submission):

"The drum was changed weekly and the exposed tape was cut into seven pieces, each one corresponding to one day, which were mounted on separate glass slides. Pollen and spores were counted under light microscope, at 600X magnification. Daily average pollen and spore counts were obtained following the standardized Spanish method (Galán et al., 2007), consisting in to run four longitudinal sweeps along the 24 h slide for daily data, identifying and counting each pollen and spore type found. To obtain the hourly concentrations, twenty-four continuous transversal sweeps separated every 2mm along the daily-sample slide, were analyzed, since the drum rotates at a speed of 2 mm per hour. Daily and intra-diurnal (hourly) pollen and spore concentrations are obtained converting the pollen and spore counts into particles per cubic meter of air, taking into account the proportion of the sample surface analyzed and the air intake of the Hirst pollen trap (10 L min^{-1})"

2. In spring, dust aerosols could be long-range transported to Barcelona. And pollen, like dust aerosols, are coarse particles and shows strong backscatter signal and large depolarization ratio from lidar measurements. Even high mass concentration of PM10 also could be seen during dust events. So the authors should explain why this is a pollination event, not a dust event. How to distinguish dust particles from pollen and spores?
Authors'reply: The synoptic situations was not favourable at all for the transport of mineral dust to Barcelona. In the Supplement 1 at the end of this document we add the forecast of mineral dust load from the BSC-DREAM8b model as well as Hysplit backtrajectories. No dust transport is forecasted by the model and the backtrajectories, identical during the five days, clearly indicate a North Atlantic (and thus clean) origin of the air masses transported to Barcelona. As Supplement 1 is not provided in the revised manuscript, the following sentence has been added at the beginning of Section 3: "To confirm that mineral dust was not transported over Barcelona during the pollination event, we used the dust transport models BSC-DREAM8b v2 (Barcelona Supercomputing Center – Dust Regional Atmospheric Model 8 bins) and NMMB/BSC-DUST (Nonhydrostatic Multiscale Meteorological Model on the B grid /

Barcelona Supercomputing Center – Dust), as well as HYSPLIT (Hybrid Single Particle Lagrangian Integrated Trajectory) backtrajectories (not shown).".

3. Page 4 line 24: incomplete sentence, "Pâ ˇ Tt' and P|| represent the perpendicular and parallel backscatter powers respectively".
Authors'reply: The sentence has been completed.

4. Page 4 line 30: please delete "linear". Strictly speaking, MPL depolarization ratio is not linear depolarization ratio.
Authors'reply: We agree with the referee that what Flynn et al. (2007) call MPL depolarization ratio, δ_{MPL}, is not the linear depolarization ratio. However the depolarization product provided by our MPL system (MPL-4B-IDS Series) is the one given in our Eq. (3), which coincides with the linear depolarization ration taking into account that $\delta_{MPL} = P_{cr} / P_{co}$ and Eq. (1.6) of Flynn et al. (2007).

5. Page 6 line 20: the authors should explain how to decide a threshold for estimating the vertical height of pollen plume. There will be better if the vertical height is estimated based on particle backscatter coefficient and depolarization ratio simultaneously.
Authors'reply: Using β_{pol} to extract the pollen top height is an estimation already based on the consideration of both the particle backscatter coefficient and the particle depolarization ratio (since both parameters are needed to retrieve β_{pol}). The value of the threshold was selected so that the integral of β_{pol} (z) up to h_{pol} represents at least 99 % of its integral over the whole column. It has been indicated with a new sentence at the end of Section 2.3: "This empirical threshold guarantees that the integral of $\beta_{pol}(z)$ up to h_{pol} represents at least 99 % of its integral over the whole atmospheric column.".

6. A peak of particle backscatter coefficient is always found at near surface (_300m), but not for depolarization ratio profiles. Overlap correction is very important before retrieval of lidar observation data, especially within boundary layer. So probably the correction is not proper, then cause this problem. Please carefully check processing of lidar data.
Authors'reply: The referee is right that overlap correction is very important. In particular for the MPL system which has a full overlap at a distance > 3 km, it is indispensable to make such a correction if ones wants to study the low troposphere. All MPL profiles shown in the paper are obviously corrected from the overlap. The overlap function used is shown in the figure thereafter. As one can appreciate, it is a very smooth function which can not produce artefacts or artificial sudden changes in the corrected lidar signals, so that we do not believe that the variation below 0.5 km are due to the overlap correction.
We had a careful look at the overall MPL data pre-processing to verify if one of the pre-processing procedures could introduce artefacts in the lidar profiles. Besides checking the overlap correction, we looked at the background subtraction, and the deadtime and afterpulse corrections. The background signal is calculated with background "bins" acquired before the laser emission. These "bins" are clearly visible before the afterpulse peak on the raw returned powers, and are guaranteed to be free of any laser-induced atmospheric signal. The deadtime correction modifies very, very little the signal in the first few hundred meters. With the naked eye, this modification is undetectable. The profile used to correct from the afterpulse effect has values different from the background signal only for heights below 100 m, and for this reason, like the overlap correction, it could not explained the differences commented by the referee.
We believe that the increase of the backscatter coefficient below 0.5 km is actually real and reflects the increase of the aerosol concentration in the surface layer in Barcelona. The fact that the depolarization ratio is not varying as much as the backscatter coefficient is not

surprising: the depolarization ratio is a semi-intensive parameter (while the backscatter coefficient is an extensive parameter) and if the main contributor to the depolarization, pollen, is well mixed and its contribution to the total aerosol load remains stable, it is to be expected that the depolarization will stay approximately constant with height. Now, the fact that the backscatter coefficient is varying while at the same time the depolarization ratio is not indicates that the increase of the backscatter coefficient is due to an equal relative increase of the concentration of both pollen and non-pollen particles.

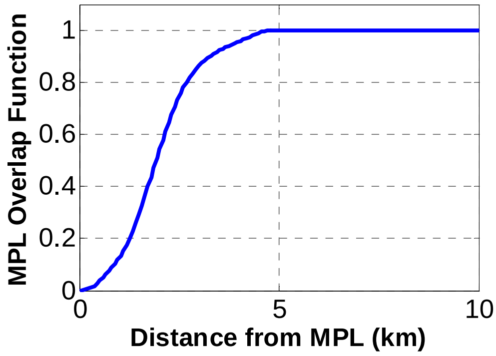

7. Page 7 line 3: add “a day” to the end of “: : :pollen and fungal spore per cubic”.
Authors’reply: It has been corrected.

8. Page 8 line 15: use abbreviation at the first time, “relative humidity (RH) and temperature (T)”.
Authors’reply: Abreviations RH and T have defined the first time they appear in the text.

9. Figure 3: why does the total pollen concentration peak precede the AOD peak of pollen? In general, high particle concentration and RH cause large AOD. However, on 31 March maximum pollen concentration and AOD were found at 3 UT and 15 UT, respectively. RH is very close but large differences between total pollen concentration (_ 2 times). Please explain the reason.
Authors’reply: Referee#1 had a similar question about this part of the manuscript. When the pollen is from local origin, not long range transport, the simple idea behind this statement is that the pollen has to be first released at ground level (concentration peak) before it disperses in the atmosphere (AOD peak). Our rationale is true only if pollen of local origin is considered, not long-range transport. This condition has been added in the text.
We have changed the two sentences starting by “As expected …” at the end of Section 3 by: “As expected, every day the AOD_{pol} peak follows the total pollen concentration peak. Logically, in the case of pollen of local origin, not long-range transport, a peak of the amount of pollen in the atmosphere (parameterized by AOD_{pol}) can only happen if previously a strong release of pollen at the ground level (parametrized by the pollen concentration) has occurred”.

10. Section 4: It is very important to fix a depolarization ratio of pollen when estimate its contribution ratio and backscatter coefficient. The authors reference results reported by other researchers. However, depolarization ratios are also affected by ambient RH. So please consider the factor and discuss uncertainty of contribution ratio and backscatter coefficient caused by artificially decided depolarization ratio.
Authors’reply: We have assessed the impact of the uncertainty of δ_{pol} on CR_{pol}. A new paragraph has been added following the discussion on the selection of δ_{pol} in Section 4. The new paragraph is:

"To assess the impact of the uncertainty of the assumed pollen depolarization ratio, δ_{pol}, on the uncertainty of the contribution ratio of the pollen to the total particle depolarization, CR_{pol}, we consider an error $\Delta\delta_{pol}$ in the pollen depolarization ratio and write:

$$CR_{pol}(z)+\Delta CR_{pol}(z)=\frac{\delta^{P}(z)-\delta_{no-pol}}{1+\delta^{p}(z)}\frac{1+\delta_{pol}+\Delta\delta_{pol}}{\delta_{pol}+\Delta\delta_{pol}-\delta_{no-pol}}, \qquad \textbf{(1)}$$

from which the relative error in CR_{pol}, $\varepsilon_{rCR_{pol}}=\frac{\Delta CR_{pol}}{CR_{pol}}$, can be found as:

$$\varepsilon_{rCR_{pol}}=-\frac{\left(1+\delta_{no-pol}\right)\Delta\delta_{pol}}{\left(1+\delta_{pol}\right)\left(\delta_{pol}-\delta_{no-pol}+\Delta\delta_{pol}\right)}. \qquad \textbf{(2)}$$

We have calculated $\varepsilon_{rCR_{pol}}$ for various values of the "true" pollen depolarization ratio ranging from 0.2 to 0.5, when $\delta_{no-pol}=0.03$ and $\delta_{pol}=0.4$ is assumed. In the range $-0.1<\Delta\delta_{pol}<+0.1$ (i.e. 0.3 < "true" pollen depolarization ratio< 0.5) the contribution ratio error is limited to ± 20 % approximately."

For the referee we are attaching thereafter the figure (not shown in the paper) showing the error $\varepsilon_{rCR_{pol}}$ as a function of the "true" pollen depolarization ratio ranging from 0.2 to 0.5, when $\delta_{no-pol}=0.03$ and $\delta_{pol}=0.4$ is assumed. Datatips indicate that for a "true" pollen depolarization ratio ranging 0.3 – 0.5, -20 < $\varepsilon_{rCR_{pol}}$ < 20 % for an assumed $\delta_{pol}=0.4$.

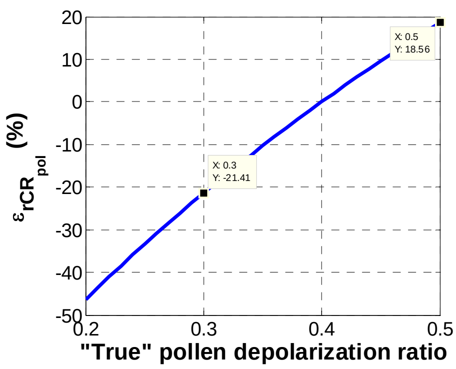

11. Page 11 line 21: The AOD is not reliable from lidar data, by integrating the profile of backscatter coefficient in the whole column and multiplying the assumed lidar ratio. Why do not use AOD from co-located AERONET sun-photometer?

Authors'reply: The referee is right: in general the AOD obtained from the integral of the backscatter coefficient profile multiplied by an assumed lidar ratio is not reliable. We can unfortunately not use co-located AERONET measurements to constrain the lidar inversion because the Barcelona AERONET sun-photometer was not in operation at the time of the pollination event. This is the reason why we had to choose a constant lidar ratio.

The selection of a proper lidar ratio (50 sr) was made given the time of year considered (March) and the type of aerosol observed (pollen). As explained at the end of Section 2.2, 50 sr falls in the range of the mean columnar lidar ratios, 46 – 69 sr, found in Barcelona during the period from February to April and calculated over a period of 3 years by Sicard et al. (2011). In that

work the columnar lidar ratio was retrieved with the two-component elastic lidar inversion algorithm constrained with the aerosol optical depth from a sun-photometer (like the referee is suggesting to do in the present work). The second reason, and probably the most grounded one, is that Noh et al. (2013b) found a mean columnar lidar ratio of 50 ± 6 sr during a 6-day pollination event (mostly dominated by *Pinus* and *Quercus* pollen) in South Korea by using the two-component elastic lidar inversion algorithm constrained with the aerosol optical depth from a sun-photometer.

12. Page 17 line 31: add "are" to ": : :lidar systems (with at least two channels) are able to produce continuously profiles: : :".
Authors'reply: The verb of this sentence is a little further. The full sentence is "First, relatively simple polarization-sensitive lidar systems (with at least two channels) able to produce continuously profiles of the volume depolarization ratio are very attractive tools for modellers to validate their pollen concentration forecasting models and/or perform data assimilation", and we believe it is correct as is.

13. Figure 2: please use particle depolarization ratio rather than volume depolarization ratio.
Authors'reply: To retrieve the particle depolarization ratio, one needs to invert the lidar signal to obtain the profile of either the backscatter or the extinction coefficient. With the Micro Pulse Lidar, which is a low energy system, such inversions typically require to average during periods of time of 1 hour. The visualization of the volume depolarization ratio with a 5-min. resolution, in opposition to 60-min. particle depolarization ratio, is an excellent way of showing qualitatively the pollen day-to-day evolution during the whole pollination event. The 60-min. profiles of the particle depolarization ratio are shown anyway in Figure 4. For these reasons, Figure 2 has been kept as a function of the volume depolarization ratio.

14. Figure 4: Too many, hard to get the points. Please 1) remove all total backscatter coefficient and volume depolarization ratio, just keep pollen backscatter coefficient and particle depolarization ratio; 2) only plot 3-4 panels per day, 9 panels are too many.
Authors'reply: To gain in readability Figure 4 has been re-formated as suggested by the referee. We have kept 4 profiles per day, every 3 hours at 9, 12, 15 and 18 UT. The profile of the particle backscatter coefficient has been removed. The profile of the volume depolarization ratio is a key parameter in the paper and for studying atmospheric pollen with a polarization-sensitive lidar system. Our study finally shows that it is almost as sensitive as the particle depolarization ratio to pollen with the advantage that its retrieval (Eq. 3 of the paper) is much more straightforward than that of the particle depolarization ratio (Eq. 4). For this reason we have wanted to keep the profile of the volume depolarization ratio in Fig. 4.

15. Figure 5: Same problem as fig 4, please remove panels of total AOD and volume depolarization ratio, and re-arrange the figure side by side.
Authors'reply: The panel of total AOD was removed from Figure 5. For the same reason given in the answer of the previous comment, the plot of the volume depolarization ratio was maintained in Figure 5.

16. Figure 6: Remove the upper panels (pollen concentration vs. volume depolarization ratio).
Authors'reply: For the same reasons given in the answer of the above two comments, we have wanted to maintain the plot of the volume depolarization ratio in Figure 6.

17. Figure 8: Depolarization ratio is used in the figure, but why do not use pollen concentration or backscatter coefficients?
Authors'reply: On request of the referee we have performed the correlation study between solar radiation and total pollen concentration and pollen AOD. In terms of correlation

coefficient it is equivalent to use the pollen AOD or the integral of the pollen backscatter coefficient profile since both properties are related by a multiplicative factor. The following figure (not included in the paper) shows the results for the total pollen concentration. The correlation coefficients range between 0.31 and 0.73, and a large scatter of the points is observed. No time delay could be found to maximize the correlation coefficients. These results point out a poor correlation between solar radiation and near-surface pollen concentration.
The correlation study between solar radiation and pollen backscatter coefficient has been included in the revised manuscript: Figure 8 has been updated as well as the discussion at the end of Section 5.

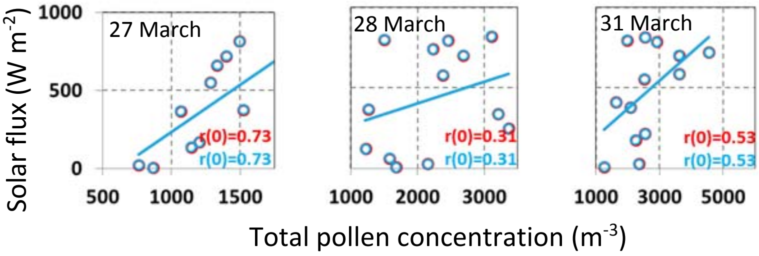

18. A paper about the vertical distribution of Asian dust measured by three MPL Lidars over Northwest China (Huang Z. et al., 2010) was published in JGR. Please reference this paper to increase reader understanding of lidar data retrieval and MPL performance. Furthermore, studies of fluorescent spectrum of atmospheric aerosols from a lidar spectrometer system with high spectral resolution (Sugimoto N. et al., 2012, OE) provides a new tools for investigating vertical structure of biological particles, which will be very useful for readers to understand remote sensing of bioaerosols.
Authors'reply: Both references have been added in the revised manuscript. Thank you for indicating them to us!

Supplement 1: BSC-DREAM8b mineral dust maps at 12UT and Hysplit backtrajectories arriving in Barcelona at 500, 1000 and 2000 m at 12UT

27 March	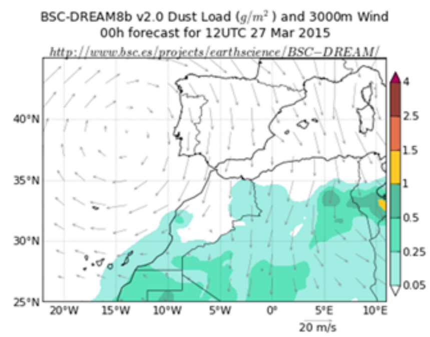	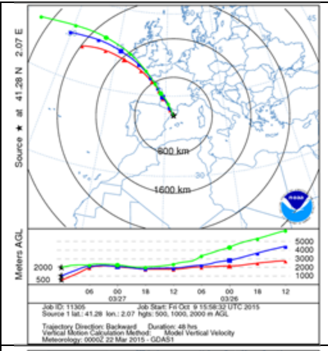
28 March	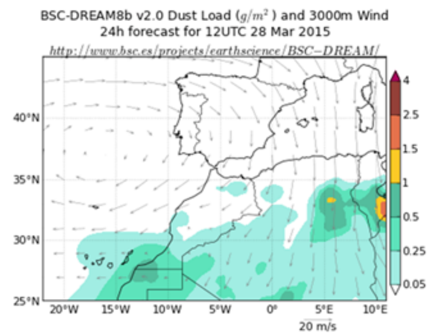	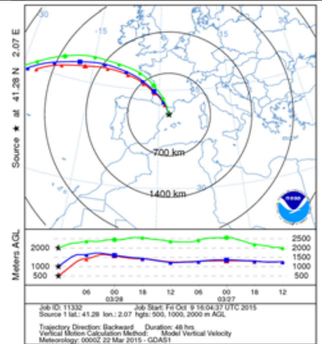
29 March	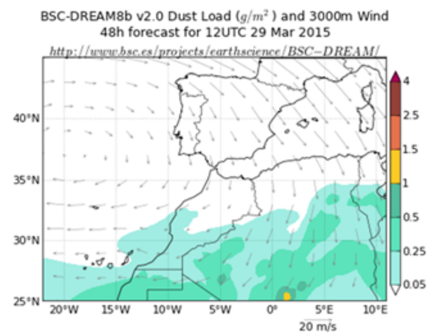	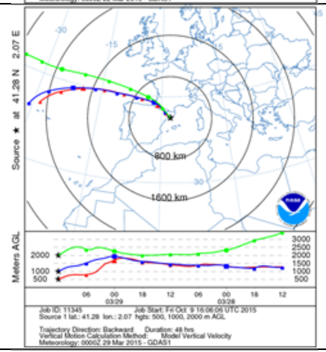
30 March	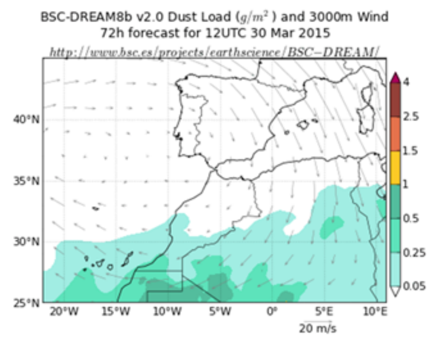	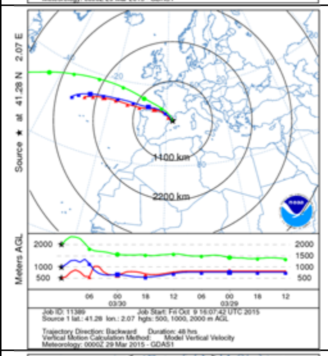
31 March	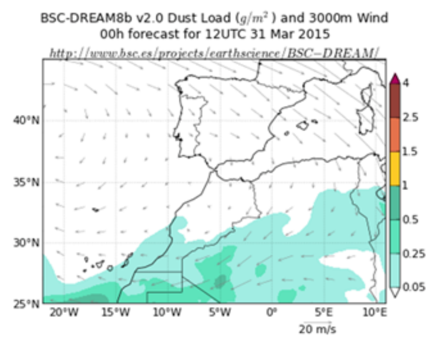	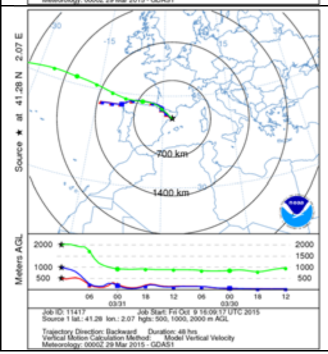

Near-surface and columnar measurements with a Micro Pulse Lidar of atmospheric pollen in Barcelona, Spain

Michaël Sicard[1,2], Rebeca Izquierdo[3], Marta Alarcón[3], Jordina Belmonte[4,5], Adolfo Comerón[1], José Maria Baldasano[6,7]

[1]Remote Sensing Laboratory, Universitat Politècnica de Catalunya, Barcelona, Spain
[2]Ciències i Tecnologies de l'Espai - Centre de Recerca de l'Aeronàutica i de l'Espai / Institut d'Estudis Espacials de Catalunya (CTE-CRAE / IEEC), Universitat Politècnica de Catalunya, Barcelona, Spain
[3]Departament de Física, Universitat Politècnica de Catalunya (UPC), c/Urgell 187, 08036 Barcelona, Spain
[4]Departament de Biologia Animal, Biologia Vegetal i Ecologia, Universitat Autònoma de Barcelona (UAB). Edifici C, 08193 Bellaterra, Spain
[5]Institut de Ciencia i Tecnología Ambientals (ICTA), Universitat Autònoma de Barcelona (UAB). Edifici Z, 08193 Bellaterra, Spain
[6]Earth Sciences Department, Barcelona Supercomputing Center – Centro Nacional de Supercomputación, Barcelona, Spain
[7]Environmental Modeling Laboratory, Technical University of Catalonia, Barcelona, Spain

Correspondence to: Michaël Sicard (msicard@tsc.upc.edu)

Con formato: Español (España)

Abstract. We present for the first time continuous hourly measurements of pollen near-surface concentration and lidar-derived profiles of particle backscatter coefficients and of volume and particle depolarization ratios during a 5-day pollination event observed in Barcelona, Spain, between 27 – 31 March, 2015. Daily average concentrations ranged 1082 – 2830 pollen m^{-3} day^{-1}. *Platanus* and *Pinus* pollen types represented together more than 80 % of the total pollen. Maximum hourly pollen concentrations of 4700 and 1200 m^{-3} h^{-1} were found for *Platanus* and *Pinus*, respectively. Everyday a clear diurnal cycle caused by the vertical transport of the airborne pollen was visible on the lidar-derived profiles with maxima usually reached between 12 and 15 UT. A method based on the lidar polarization capabilities was used to retrieve the contribution of the pollen to the total aerosol optical depth (AOD). On average the diurnal (9 – 17 UT) pollen AOD was 0.05 which represented 29 % of the total AOD. Maximum values of the pollen AOD and its contribution to the total AOD reached 0.12 and 78 %, respectively. The diurnal means of the volume and particle depolarization ratios in the pollen plume were 0.08 and 0.14, with hourly maxima of 0.18 and 0.33, respectively. The diurnal mean of the height of the pollen plume was found at 1.24 km with maxima varying in the range 1.47 – 1.78 km. A correlation study is performed 1) between the depolarization ratios and the pollen near-surface concentration to evaluate the ability of the former parameter to monitor pollen release, and 2) between the depolarization ratios as well as pollen AOD and surface downward solar fluxes, which cause the atmospheric turbulences responsible for the particle vertical motion, to examine the dependency of the depolarization ratios and the pollen AOD upon solar fluxes. For the volume depolarization ratio the first correlation study yields to correlation coefficients ranging 0.00 – 0.81 and the second to correlation coefficients ranging 0.7049 – 0.86.

1. Introduction

Pollen is the male gametophyte of seed plants. Both gymnosperms (cone-bearing plants) and angiosperms (flowering plants) produce pollen as part of sexual reproduction. Pollen grains have characteristic walls with distinctive ornamentation that permit their identification. The production and emission of pollen are governed by interacting environmental factors, as photoperiod, temperature and water stress (Dahl et al, 2013). Pollen is primarily dispersed in the atmosphere by insects or wind. Wind-pollinated plants are called anemophilous and they produce huge amounts of pollen grains which, once airborne, are responsible of allergenic reactions when inhaled by humans (Cecchi, 2013). Fungal spores are a biological component that can be found any time of the year in the atmosphere (Lacey, 1981; Burch and Levetin, 2002). Environmental variables, such as temperature and moisture, can influence growth and reproduction in fungi which makes airborne spore concentrations to fluctuate seasonally (Grinn-Gofrón and Strzelczak, 2008; Pakpour et al., 2015). However, it has also been observed that local climate, vegetation patterns and management of landscape are governing parameters for the overall spore concentration, while the annual variations caused by weather, although not negligible, are of secondary importance (Skjøth et al., 2016). Fungi are, after pollen, the second most important producers of outdoor airborne allergens (Weikl et al., 2015). Their presence can cause human health problems (mainly allergies) and crop infections (phytopathology) (e.g. Burge and Rogers, 2000; Simon-Nobbe et al., 2008). Up to 80 % of asthmatics are sensitized to fungal allergens (Lopez and Salvaggio, 1985) and a disease pattern of severe asthma with fungal sensitization has been recently proposed (Denning et al., 2006).

Worldwide many people living in large cities suffer from allergies linked to the presence of atmospheric pollen and fungal spores. In the industrialized countries of central and northern Europe, up to 15 % of the population is sensitive to pollen allergens (WHO, 2003; Cecchi, 2013). In Europe the most common types of pollen are *Ambrosia*, *Alnus*, *Artemisia*, *Betula*, *Corylus*, Chenopodiaceae, Cupressaceae/Taxaceae, *Olea*, *Platanus*, Poaceae, *Quercus*, and *Urtica*/*Parietaria* (Skjøth et al. 2013). Although their concentration is monitored daily at ground level by aerobiological networks (Scheifinger et al., 2013, Karatzas et al., 2013), very little is known on their vertical distribution and their long/short range transport (Sofiev et al., 2013) although an increase interest has arisen very recently in the aerosol lidar community (Sassen, 2008; Noh et al., 2013a; 2013b). Sassen (2008) reported on lidar measurements in the lower atmosphere of birch pollen plumes from the boreal forest of Alaska. Noh et al. (2013a) retrieved optical properties with a polarization-sensitive lidar for *Pinus* and *Quercus* pollen in South Korea. Noh et al. (2013b) reported on the vertical distribution of the same pollen event observed with lidar and on the dependency of its diurnal variations upon the meteorological conditions (temperature, relative humidity, and wind speed). Sugimoto et al. (2012) developed a lidar spectrometer system with high spectral resolution which showed promising results for investigating the vertical structure of biological particles.

Con formato: Fuente: (Predeterminada) Times New Roman, 10 pto

Con formato: Fuente: (Predeterminada) Times New Roman, 10 pto

Con formato: Fuente: (Predeterminada) Times New Roman, 10 pto

In the Mediterranean city of Barcelona, Spain, the most abundant pollen taxa are *Quercus* (27,4 % of the total pollen), *Pinus*, *Platanus*, Cupressaceae, *Olea*, Urticaceae, Poaceae, Chenopodiaceae, *Plantago*, Moraceae, *Fraxinus*, *Castanea* and *Populus* (1 %) according to the Aerobiological Network of Catalonia (http://lap.uab.cat/aerobiologia) and based on pollen concentrations measured in the period 1994-2015. Barcelona is the Spanish city which presents the longest mean pollen season of *Platanus* pollen. Maximum daily counts occur generally during the second half of March (Díaz de la Guardia et al., 1999). *Platanus hispanica* is responsible of the most frequent pollen sensitizations (37 %) detected in Barcelona (Puiggròs et al, 2015). *Pinus* is one of the most abundant pollen taxa in Spain (Belmonte and Roure, 1991; De Linares et al. 2014). In Barcelona *Pinus* pollination occurs in two phases, the most important one happens from March to May and the other in June-July. Regarding airborne fungal spores, *Cladosporium* is the most abundant taxon in Barcelona, representing up to 44% of the total fungal spore spectrum. It is present all year round, and shows the highest concentrations in April-May and November (Infante et al., 1999; see also http://lap.uab.cat/aerobiologia). This paper aims at investigating the possible correlation between pollen near-surface concentration and columnar properties measured during a 5-day pollination event in Barcelona. The dataset is composed of continuous measurements at a temporal resolution of one hour. The influence of the meteorological conditions and the solar radiation on the pollen dispersion is also investigated. This contribution relates for the first time near-surface and lidar measurements of pollen in a large European city.

The paper is organized as follows: Section 2 presents the methods used to count the pollen and spore taxa and also describes the lidar instrument used and the method employed to estimate the pollen optical properties. Pollen and spores measured in Barcelona are first analyzed with daily mean concentration values and lidar quicklooks (time-altitude contour plots) in Section 3. The analysis of the temporal evolution of hourly concentrations and meteorological parameters completes this Section. Section 4 is dedicated to the investigation of possible correlations between near-surface pollen concentration and the vertical distribution of a series of structural and optical properties. Finally Section 5 enlightens us on the relationship between the vertical transport of airborne pollen and the solar radiation.

2. Instrumentation and method

2.1. Pollen and spores sampling instrumentation, PM_{10} and meteorological data

Airborne pollen and spore data were collected by the Aerobiological Network of Catalonia at the sampling station situated on the roof of a building in the city centre of Barcelona (2.164º E, 41.394° N). Samples were obtained using volumetric suction pollen-spore trap based on the impact principle (Hirst, 1952), the standardized method in European aerobiological networks. The Hirst sampler is calibrated to handle a flow of 10 litre of air per minute, thus matching the human breathing rate. Pollen and spores are impacted on a cylindrical drum covered by a melinex film coated with a 2-% silicon solution as trapping surface. The drum was changed weekly and the exposed tape was cut into seven pieces, each one corresponding to one day, which were mounted on separate glass slides. Pollen and spores were counted under light microscope, at 600X magnification. Daily average pollen and spore counts were obtained following the standardized Spanish method (Galán et al., 2007), consisting in running four longitudinal sweeps along the 24 h slide for daily data, identifying and counting each pollen and spore type found. To obtain the hourly concentrations, twenty-four continuous transversal sweeps separated every 2 mm along the daily-sample slide, were analyzed, since the drum rotates at a speed of 2 mm per hour. Daily and intra-diurnal (hourly) pollen and spore concentrations are

Con formato: Fuente: Sin Negrita

Con formato: Fuente: Sin Negrita

Con formato: Fuente: Sin Negrita

Con formato: Fuente: Sin Negrita

Con formato: Fuente: Sin Negrita

obtained converting the pollen and spore counts into particles per cubic meter of air, taking into account the proportion of the sample surface analyzed and the air intake of the Hirst pollen trap (10 L min^{-1}).

Con formato: Fuente: Sin Negrita
Con formato: Superíndice
Con formato: Fuente: Sin Negrita

The drum was changed weekly and the exposed tape was cut into seven pieces, which were mounted on separate glass slides. Pollen and spores identification was performed using a microscope equipped with a 40X/15 lens. Daily average and diurnal (hourly) pollen and spore concentrations were made following the standardized Spanish method (Galán et al., 2007), consisting in: (1) four continuous longitudinal sweeps along the 24 h slide for daily data, which gives a subsample accounting for 12-13% of the total surface; and (2) twenty-four continuous transversal sweeps separated every 2mm along the daily-sample slide, since the tape rotates 2 mm every hour, for hourly data. Pollen and spore concentrations and diurnal variations (hourly concentrations) were expressed as the number of pollen grains and spores per cubic meters of air.

PM_{10} measurements were acquired at the "Eixample" station of the Xarxa de Vigilància i Previsió de la Qualitat de l'Aire (XVPCA, the Catalonian network for monitoring and forecasting the air quality). It is located at 1.2 km to the southwest of the pollen sampling instrumentation.

Meteorological data were recorded in the "Zona Universitaria" area of Barcelona, at approximately 0.6 km south-southeast of the lidar site.

2.2. The Barcelona Micro Pulse Lidar

The profiles of the particle backscatter coefficient and the particle depolarization ratio were measured with the Barcelona Micro Pulse Lidar (MPL) system, model MPL-4B. The system is located in the "Zona Universitaria" area of the city, on the roof of the Remote Sensing Lab (RSLab) building in the North Campus of the Universitat Politècnica de Catalunya (2.112º E, 41.389º N, 115 m a.s.l.), approximately 1 km from Sierra de Collserola and 7 km from the sea. It is located at 4.4 km to the west of the pollen sampling instrumentation. The system should become very shortly part of the MPLNET (Micro Pulse Lidar Network, http://mplnet.gsfc.nasa.gov/) network. The MPL system is a compact, eye-safe lidar designed for full-time unattended operation (Spinhirne, 1993; Campbell et al., 2002; Flynn et al., 2007; Huang et al., 2010). It uses a pulsed solid-state laser emitting low laser pulse energy (~6 μJ) at a high pulse rate (2500 Hz) and a co-axial "transceiver" design with a telescope shared by both transmit and receive optics. The Barcelona MPL optical layout uses an actively controlled liquid crystal retarder which makes the system capable to conduct polarization-sensitive measurements by alternating between two retardation states (Flynn et al., 2007). The signals acquired in each of these states are recorded separately and called "co-polar" and "cross-polar". In nominal operation the raw temporal and vertical resolutions are 30 s and 15 m, respectively.

The linear volume depolarization ratio, δ^V, is defined as:

$$\delta^V(z) = \frac{\beta_\perp(z)}{\beta_\parallel(z)} = \frac{P_\perp(z)}{P_\parallel(z)} \tag{1}$$

where $\beta_\perp$ and $\beta_\parallel$ denote the total (particles + molecules) perpendicular and parallel backscatter coefficient, respectively, and $P_\perp$ and $P_\parallel$ represent the perpendicular and parallel backscatter powers, respectively. According to Gimmestad (2008) δ^V can also be expressed as a function of a factor *d* which has a range of 0–1 and which is related to the propensity of the scattering medium to preserve the incident polarization:

$$\delta^V(z) = \frac{d}{2-d} \tag{2}$$

In the case of a linear polarization lidar, *d* = 0 indicates that no depolarization occurs, while *d* = 1 indicates that the returned beam is completely depolarized. By adapting the notations of Flynn et al. (2007), especially in Eqs (1.4) and (1.6), to ours one can formulate the linear volume depolarization ratio for the MPL system as:

$$\delta^V(z) = \frac{P_{cr}(z)}{P_{co}(z) + P_{cr}(z)} \tag{3}$$

where P_{cr} and P_{co} represent the MPL cross- and co-polar channels, respectively.

The linear particle depolarization ratio, δ^p, can then be determined by (Freudenthaler et al., 2009):

$$\delta^p(z) = \frac{\beta_\perp^p(z)}{\beta_\parallel^p(z)} = \frac{\left[1+\delta^m\right]\delta^V(z)R(z) - \left[1+\delta^V(z)\right]\delta^m}{\left[1+\delta^m\right]R(z) - \left[1+\delta^V(z)\right]} \tag{4}$$

where $\beta_\perp^p$ and $\beta_\parallel^p$ are the particle perpendicular and parallel backscatter coefficients, respectively, δ^m is the molecular depolarization ratio and *R* is the backscatter ratio which is defined as:

$$\mathrm{R}(z) = \frac{\beta^m(z) + \beta^p(z)}{\beta^m(z)} \tag{5}$$

where β^m and β^p denote the molecular and particle backscatter coefficient, respectively, of the total (perpendicular + parallel) returned signal. According to the MPL optical requirements in the receiving system the spectral filtering is performed by filters with a spectral band ≤ 0.2 nm. This number produces a temperature-independent molecular depolarization ratio of $\delta^m = 0.00363$ according to Behrendt and Nakamura (2002).

The particle backscatter coefficient, β^p, was retrieved with the two-component elastic algorithm (also known as the Klett-Fernald-Sasano method; Fernald, 1984; Sasano and Nakane, 1984; Klett, 1985) with a constant lidar ratio of 50 sr and applied to the total lidar signal, P, reconstructed from the MPL lidar signals as (Flynn et al., 2007):

$$P(z) = P_{co}(z) + 2P_{cr}(z) \tag{6}$$

The value of 50 sr is motivated by two previous studies. First, it falls in the range of the mean columnar lidar ratios, 46 – 69 sr, found in Barcelona during the period from February to April and calculated over a period of 3 years (Sicard et al., 2011). In that work the columnar lidar ratio was retrieved with the two-component elastic lidar inversion algorithm constrained with the aerosol optical depth from a sun-photometer (Landulfo et al., 2003; Reba et al., 2010). Second, Noh et al. (2013b) used the same method and found a mean columnar lidar ratio of 50 ± 6 sr during a 6-day pollination event (mostly dominated by *Pinus* and *Quercus* pollen) in South Korea. At the peak of the event the pollen aerosol optical depth (AOD) represented up to 35 % of the total AOD.

2.3. Determination of pollen optical and structural properties

Pollen has formerly been distinguished from other particle types thanks to its depolarization capabilities (Sassen, 2008; Noh et al., 2013a; 2013b). Although many types of pollen have regular shapes (circular, spherical, elliptical, ovoid, etc.), they cannot be considered spherical from the point of view of light scattering because they do not generate Mie patterns expected from a sphere of equivalent size. The reason lies in surface imperfections of pollen grains and inhomogeneous refractive indices inside the grains

When the atmospheric particle load can be assumed as the external mixing of one type of depolarizing particles (the pollen, here) with another type of much less ~~non-~~depolarizing particles, the method suggested by Shimizu et al. (2004) allows to separate the contribution ratio of both types of particles. The same rationale leading to Eq. (4) allows to define a ~~In our case, the~~ pollen (highly depolarizing particles) contribution ratio to the total particle depolarization ratio, CR_{pol} , ~~can be~~ expressed as:

$$CR_{pol}(z) = \frac{\left[\delta^{p}(z) - \delta_{no-pol}\right]\left[1 + \delta_{pol}\right]}{\left[\delta_{pol} - \delta_{no-pol}\right]\left[1 + \delta^{p}(z)\right]} \tag{7}$$

where δ_{no-pol} and δ_{pol} are the particle depolarization ratios of all particle types except pollen (weakly ~~non-~~depolarizing) and the pollen (depolarizing), respectively. One can check easily that if no pollen is present $\delta^{p} = \delta_{no-pol}$ and Eq. (7)~~(7)~~ leads to $CR_{pol} = 0$, and that if only pollen is present $\delta^{p} = \delta_{pol}$ and Eq. (7)~~(7)~~ leads then to $CR_{pol} = 1$. The pollen backscatter coefficient, β_{pol} , is simply calculated as:

$$\beta_{pol}(z) = CR_{pol}(z)\beta^{p}(z) \tag{8}$$

The contribution ratio is sensitive to the selection of δ_{no-pol} and δ_{pol} which are determined either empirically or taken from references. To fix the value of δ_{no-pol} we searched for a clear-sky day prior to the pollination event without long-range transport aerosols. Such conditions were fulfilled on 15 March around 12 UT. On that day a well-mixed atmospheric boundary layer (ABL) developed. At 12 UT the ABL height was ~1.2 km and the AOD 0.18. The particle depolarization ratio was constant ~0.03 in the whole ABL. We have taken $\delta_{no-pol} = 0.03$. In the literature very few information on measurements of pollen depolarization ratios is available. The choice of δ_{pol} is deferred to Section 4, after the analysis of the individual profiles of δ^{p} , in order to have as much information as possible. A short discussion on the uncertainty of CR_{pol} and β_{pol} linked to the choice of δ_{pol} is also discussed in Section 4.

Finally we also calculated the vertical height, h_{pol} , up to which the pollen plume extends. As it is shown in Section 4, the pollen plume is characterized during the whole pollination event by a near-constant or slightly decreasing profile of β_{pol} . From this aspect the structure of the pollen plume is much simpler than the ABL structure usually found in Barcelona (Sicard et al., 2006). This allows us to use a simple threshold method such

Con formato: Inglés (Estados Unidos)

Código de campo cambiado

Código de campo cambiado

Código de campo cambiado

as the one used to estimate the ABL height by Melfi et al. (1985) and Boers et al. (1988). After several tests we empirically set a threshold of 0.055 Mm^{-1} sr^{-1} and defined h_{pol} as the ~~first~~ height at which $\beta_{pol}(z) < 0.055\ Mm^{-1} sr^{-1}$. This empirical threshold guarantees that the integral of $\beta_{pol}(z)$ up to h_{pol} represents at least 99 % of its integral over the whole atmospheric column.

Código de campo cambiado

Código de campo cambiado

3. Temporal variation of pollen and spore taxa near-surface and columnar properties

In the second half of March 2015 a strong anticyclone positioned in the Atlantic Ocean west of the Portuguese coast generated northwe~~southea~~sterly winds in the northeastern part of the Iberian Peninsula. In Barcelona, the synoptic conditions resulted in marked, off-shore winds in altitude yielding to relatively clear skies and preventing long-range transport of highly depolarizing aerosols like mineral dust over Barcelona. To confirm that mineral dust was not transported over Barcelona during the pollination event, we used the dust transport models BSC-DREAM8b v2 (Barcelona Supercomputing Center – Dust Regional Atmospheric Model 8 bins) and NMMB/BSC-DUST (Nonhydrostatic Multiscale Meteorological Model on the B grid / Barcelona Supercomputing Center – Dust), as well as HYSPLIT (Hybrid Single Particle Lagrangian Integrated Trajectory) backtrajectories (not shown).

Con formato: Fuente: Sin Negrita

Ninety three pollen types and forty fungal spore types are counted routinely on a daily basis at the Aerobiological Network of Catalonia. The daily variation of the concentration of the four most abundant pollen (*Platanus, Pinus* and Cupressaceae) and spore (*Cladosporium*) taxa and the total (pollen + spore) is represented in Figure 1~~Figure 1~~a for a period surrounding the peak of the pollination event under study. Figure 1~~Figure 1~~b shows the fraction of each one of the four most abundant taxa to the total (pollen + spore). During the pollination event, 26 – 31 March, the total concentration varies between 1082 and 2830 pollen and fungal spore per cubic meter a day. Three days before (23 March) and after (3 April) the event, values of 275 and 368 m^{-3} ~~day^{-1}~~ are registered, respectively. The most abundant taxon is *Platanus* which represents between 48 – 71 % of the total concentration during the pollination event. This range of values is higher than the annual fraction of *Platanus* to total pollen, 46.3 %, estimated by Gabarra et al. (2002) over the period 1994 – 2000 in the city of Barcelona. The *Platanus* daily concentration reaches a maximum of 1703 m^{-3} ~~day^{-1}~~ on 31 March. This value is in the lower part of the range of daily maxima (1543 – 2567 m^{-3} ~~day^{-1}~~) observed per year over the period 1994 – 2000 by Gabarra et al. (2002). *Pinus* is the second most abundant taxon which represents between 18 and 30 % of the total concentration during the pollination event and reaches a maximum of 803 m^{-3} ~~day^{-1}~~ on 30 March. During the whole event *Platanus* and *Pinus* pollen types represent 80 % or more of the total concentration. *Pinus* is the taxon that presents the highest relative increase since its fraction passes from values lower than 10 % before the event to up to values ranging in 18 -30 % during the event. The third most abundant taxon is *Cladosporium* spore which represent between 6 and 11 % of the total concentration during the pollination event and reaches a maximum of 224 m^{-3} ~~day^{-1}~~ on 31 March. This value is of the order of magnitude of the daily means observed during the month of March (~ 200 m^{-3} ~~day^{-1}~~) by Infante et al. (1999) over a 6-year period in the city of Barcelona. Finally the fourth most abundant taxon is Cupressaceae which does not count for more than 5.4 % (on 27 March)

Con formato: Fuente: 10 pto

Con formato: Fuente: 10 pto

of the total concentration. With a maximum peak of 74.9 m^{-3} ~~day^{-1}~~ (on 28 March), this event is of rather low intensity for Cupressaceae as it falls at the end of the pollen season for that taxon according to Belmonte et al. (1999).

The temporal evolution of the profiles of the particle backscatter coefficient and the volume linear depolarization ratio during the pollination event is shown in Figure 2~~Figure 2~~. Aerosols are present everyday up to 2.5 – 3 km. However most of the aerosol load is found below approximately 1.5 km. Near the ground (< 0.5 km) high values of β^p (4 Mm^{-1} sr^{-1}) are found on almost all days. Between 0.5 and 1.5 km the green color code indicates values of β^p not higher than 2 – 2.5 Mm^{-1} sr^{-1} (except on 26 March on which day clouds are present below 2 km before 08 UT). In general two regimes are observed everyday: an increase in amplitude and height starting around 10 UT which persists until the night, and a less pronounced nighttime regime starting usually after midnight. On 31 March one sees a layer appearing after 11 UT with very large values of β^p (> 5 Mm^{-1} sr^{-1}) and confined in the first 0.5 km of the ABL. This increase of β^p in the bottom part of the ABL has no impact on the volume depolarization ratio vertical distribution (Figure 2~~Figure 2~~b) which suggests that it is due to non-depolarizing particles. The green color code volume depolarization ratio shown in Figure 2~~Figure 2~~b indicates values of δ^V near 0.02 – 0.03. It is the usual value of δ^V for background, local aerosols near the surface in Barcelona. Everyday around 08 UT a plume with δ^V > 0.08 (yellowish) appears, raises up to 1.0 – 1.7 km in a few hours and starts decreasing before 16 UT at a lesser rate than it raised. This diurnal pattern of δ^V is observed on each single day of the pollination event. On the first four days values of δ^V larger than 0.08 are no longer detected after 18 – 20 UT. Toward the end of the event on 30 and 31 March when the pollen concentrations were the highest values of δ^V > 0.08 are still detected until 21-24 UT. The highest values of δ^V are detected on 30 March and are of the order of 0.22. This maximum value is higher than the peak value of 0.15 observed by Noh et al. (2013b) for *Pinus* and *Quercus* pollen in South Korea and lower than δ^V = 0.30 measured by Sassen (2008) for birch pollen plumes from the boreal forest of Alaska.

Because of the presence of clouds near the ABL top in the first part of 26 March (Figure 2~~Figure 2~~b), this day is discarded in the rest of the paper and from now on we will focus only on the period 27 – 31 March. To gain an insight into the temporal variations of the pollen and spore taxa concentration we performed for the period 27 – 31 March a counting on an hourly basis. The method used is described in Section 2.1. Although all pollen and spore taxa were counted, in the following we will only show the results of the total pollen (spore is no longer taken into account) and of the two most abundant pollen types: *Platanus* and *Pinus*. The two main reasons for that choice are that 1), as found earlier, *Platanus* and *Pinus* pollen represent more than 80 % of the total (pollen + spore) taxa and 2) the ratio of total spore to total pollen is less than 13 % during the period 27 – 31 March.

Many works have investigated the influence of the meteorological conditions, such as relative humidity (RH), temperature (T), wind speed, the number of sunshine hours and rainfall, on the release and transport of pollen in the atmosphere (Raynor et al., 1973, Mandrioli et al., 1984; Hart et al., 1994; Alba et al., 2000; Jato et al., 2000; Bartková- Ščevková, 2003; Vázquez et al., 2003; Latorre and Caccavari, 2009, among others). On the one hand, relative humidity and temperature greatly affect the release of pollen in the atmosphere by influencing the extent to which individual pollen grains dehydrate. For example a low relative humidity associated with a high temperature will tend to increase the number of airborne pollen grains by decreasing their specific gravity.

Con formato: Fuente: 10 pto, Sin Negrita

Con formato: Fuente: 10 pto, Sin Negrita

Con formato: Fuente: 10 pto, Sin Negrita

Con formato: Fuente: 10 pto, Sin Negrita

The relation of pollen with water comes from its hydrophilic properties and from the fact that it is prone to harmomegathic movement (accommodation of volume change when it absorbs water; Wodehouse, 1935). The duration of the sunshine has also proved to have an influence on the pollen release (Alba et al., 2000). On the other hand, wind speed plays a major role in the transport and dispersion of airborne pollen: high daytime wind speed may facilitate the dispersion of airborne pollen in the atmosphere (Latorre and Caccavari, 2009; and references therein). The effect of rainfall is to reduce the number of airborne pollen grains by washing out the atmosphere. During the pollination event presented in this work, no rain was detected.

In Figure 3~~Figure 3~~ we present the hourly temporal variations of 1) *Platanus*, *Pinus* and total pollen concentration during the period 27 – 31 March, together with 2) relative humidity ~~(RH)~~, 3) temperature ~~(T)~~ and 4) wind speed. In Figure 3~~Figure 3~~b we also indicated the time of the maximum pollen concentration and pollen AOD on each day. The pollen AOD, AOD_{pol}, was obtained by integrating the profile of β_{pol} from the ground up to h_{pol} and multiplying the result by the same lidar ratio used in the lidar inversion, 50 sr (see Section 2.2).

With the exception of 31 March, the pollen number concentration at ground level follows a clear diurnal cycle (Figure 3~~Figure 3~~a). On 31 March, no clear difference is observed between day and night. *Platanus* and *Pinus* concentration reaches maximum peaks of ~4700 m^{-3} ~~h^{-1}~~ on 31 March and 1200 m^{-3} ~~h^{-1}~~ on 30 March, respectively. Maximum peaks of the total pollen concentration higher than 5000 and 6000 m^{-3} ~~h^{-1}~~ are reached on 30 and 31 March, respectively. They are associated with absolute peaks of *Platanus* and relative peaks of *Pinus*. Interestingly a release cycle is visible each day: the diurnal variation is marked with several relative peaks along the day that are usually distant in time by 2 to 4 hours. *Platanus* and *Pinus* peaks are not necessarily correlated. The fact that *Platanus* variations are shaper than *Pinus* ones may be explained by the size difference between both pollen types: while *Platanus* longest diameter (on the polar axis) varies between 21 and 28 µm, it varies between 60 and 74 µm for *Pinus* (https://www.polleninfo.org/AT/en/allergy-infos/aerobiologics/pollen-atlas.html?letter=P). Pollen size is known to be a factor affecting pollen release but also their settlement to the ground (McCartney, 1994).

The relative humidity and temperature hourly evolution shows a clear diurnal cycle (Figure 3~~Figure 3~~b): a relative humidity decrease associated with a temperature increase is observed during daytime while the opposite occurs during nighttime. Daytime RH (T) values are found in the range of 40 – 60 % (17 – 25 ºC) while nighttime values are found in the range of 65 – 90 % (12 – 18 ºC). While no marked trend is observed on the relative humidity along the pollination event, a temperature day-to-day increase is observed, the daily mean temperature passing from 15.2 – 17.5 – 16.6 – 18.5 to 17.9 ºC between 27 and 31 March. The correlation coefficient between the daily mean temperature and the daily total pollen concentration is 0.95, indicating a strong dependence of pollen release upon temperature. The correlation coefficient between the daily mean relative humidity and the daily total pollen concentration, -0.18, is negative but much lower (in absolute value) than the one for temperature. Except on 28 and 31 March (when wind speeds higher than 6 m s^{-1} are detected in the first half of the day), the daytime wind speed usually oscillated between 2 and 3 m s^{-1} (with gusts at ~4.5 m s^{-1}) which corresponds to a light breeze. From 27 to 31 March, the daily wind speed varies from 1.6 – 2.5 – 1.5 – 3.7 to 2.4 m s^{-1}, similarly to the daily mean temperature. The correlation coefficient between daily wind

Con formato: Fuente: 10 pto, Sin Negrita

Con formato: Fuente: 10 pto, Sin Negrita

Con formato: Fuente: 10 pto, Sin Negrita

Con formato: Fuente: 10 pto, Sin Negrita

speed and total pollen concentration is 0.82, indicating a strong dependence of pollen release also upon wind speed.

Each day the time of the maximum peak of the total pollen concentration (red vertical lines, Figure 3~~Figure 3~~b) occurs between 02 and 11 UT, while that of AOD_{pol} (grey vertical lines, Figure 3~~Figure 3~~b) occurs more regularly between 12 and 15 UT. As expected, every day the ~~total pollen concentration peak precedes the~~ AOD_{pol} peak follows the total pollen concentration peak. Logically, in the case of pollen of local origin, not long-range transport, ~~a~~ a peak of the amount of pollen in the atmosphere (parameterized by AOD_{pol}) can only happen if previously a strong release of pollen at the ground level (parametrized by the pollen concentration) has occurred~~at a given time is chronologically followed by a peak of the amount of pollen in the atmosphere, here parameterized by the pollen AOD, when the conditions for the dispersion of pollen in the atmosphere are gathered~~. On the one hand and surprisingly the total pollen concentration peaks are not systematically associated with minima of RH, maxima of T and/or of the wind speed, while, on the other hand, the pollen AOD peaks are systematically associated with minima of RH and maxima of T. The pollen AOD peaks do not present a systematic dependence upon wind speed, a result in agreement with the findings of Noh et al. (2013a) who showed a broad variation of the pollen AOD for wind speeds lower than 3 m s^{-1}.

4. Pollen near surface vs. columnar properties: day-by-day analysis

The daily temporal variation of some lidar-derived range-resolved and columnar parameters are investigated and further compared to pollen concentrations in order to find possible correlations. Figure 4~~Figure 4~~ shows the diurnal (9 – 1~~7~~8 UT) profiles of the ~~particle and~~ pollen backscatter coefficients and of the volume and particle linear depolarization ratios for the 5 days of the event. The top height of the pollen plume, h_{pol}, is also indicated in the plots by horizontal grey lines. The profiles of δ^V are characterized by a near-constant or slightly decreasing slope with increasing height which reaches zero generally sharply at h_{pol}. The profiles of δ^p, which unlike δ^V show only the particle depolarization effect, have a general tendency to decrease with increasing height, reflecting the gradual diminution of the number of pollen as height increases. It is also frequent to find $\delta^p > 0.2$, especially at the beginning of the day, in the lowermost part of the ABL (below 0.3 km) where most of the pollen grains concentrate.

Maxima of δ^V of the order of 0.22 are reached on 30 March at 12 UT below 0.75 km. On that particular profile, some values of δ^V are associated with comparatively low values of β^p (< 2 Mm^{-1} sr^{-1}~~)~~, not shown), and therefore with low values of the backscatter coefficient R which altogether contribute to increase δ^p according to Eq. (4)~~(4)~~. This produced values of δ^p in the range of 0.40 – 0.43 at the height of 0.5 km. Other maxima of δ^p of 0.35 are observed on 30 March at 11 UT, and of 0.31 on 29 and 30 March at 12 and 13 UT, respectively, all at the same height of ~0.5 km. With this in mind we now come back to the choice of δ_{pol} needed for

Con formato: Fuente: 10 pto, Sin Negrita

Con formato: Fuente: 10 pto, Sin Negrita

Con formato: Subíndice

Con formato: Fuente: 10 pto, Sin Negrita

applying Shimizu's method and left in stand-by in Section 2.3. Very few information is available on that subject (in chronological order):

- Sassen (2008) found maxima of δ^V of 0.30 for birch pollen plumes from the boreal forest of Alaska that he described as "unusually high for aerosols, and […] comparable to irregularly-shaped desert dust particles raised by dust storms". This finding implies that $\delta^p > 0.30$ in the pollen cloud he observed.
- In two consecutive papers Cao et al. (2010) and Roy et al. (2011) measured the linear particle depolarization at four wavelengths of several types of pollen in an aerosol chamber with a polarization-sensitive lidar. For *Pinus* (*Platanus* was not tested) they found a mean δ_{pol} of 0.41 and 0.42, respectively.
- Noh et al. (2013a) used Shimizu's method with a pollen depolarization ratio equal to that of pure mineral dust, $\delta_{pol} = 0.34$, without further justification.
- Noh et al. (2013b) found a maximum value of δ^p of 0.23 in a cloud of *Pinus* and *Quercus* pollen mixed with local aerosols (urban haze) in South Korea. Although they used a definition of the particle depolarization ratio different from ours, we corrected the maximum value found in their paper with their Eq. (2) in order to make $\delta^p = 0.23$ compatible with our definition. Given their estimation of urban haze depolarization ratio, 0.03, the value of $\delta^p = 0.23$ implies $\delta_{pol} \geq 0.23$.
- In the present study we found maxima of δ^p of 0.31, 0.35 and 0.43 in a cloud of *Platanus* and *Pinus* pollen mixed with local urban aerosols. Given our estimation of the local, urban aerosol depolarization ratio, 0.03 (see Section 2.3), the former rationale implies that δ_{pol} might be greater than 0.43, error bars apart.

It is worth noting that the maximum value of δ^p of 0.43 observed on 30 March at 12 UT coincides in time with the lowest relative humidity and the highest temperature observed during the whole pollination event (see Figure 3~~Figure 3~~b). We have checked that the relative humidity and temperature profiles (not shown) measured daily by radiosoundings launched close to the lidar site were, respectively, the lowest (RH < 40 % up to 1 km) and the highest (T > 15ºC up to 1 km) on 30 March at 12 UT. It also follows a strong peak of pollen release at ground level at 09 UT (Figure 3~~Figure 3~~a) that occurred at the end of an 8-hour period of strong winds of 6 to 10 m s^{-1} that might have partially cleaned the atmosphere. All in all it is reasonable to think that the aerosol load on 30 March at 12 UT in the first kilometre may be composed of quasi-pure pollen. Another point to take into account is the error bar associated to the calculation of the MPL particle linear depolarization ratio. To have an estimation of this error we calculated the standard deviation of the 120 profiles that composed the 1-hour averaged profile shown in Figure 4~~Figure 4~~. For the measurement of 30 March at 12 UT we find a standard

Con formato: Fuente: 10 pto, Sin Negrita

Con formato: Fuente: 10 pto, Sin Negrita

Con formato: Fuente: 10 pto, Sin Negrita

deviation of 0.02 at 0.5 km and of 0.08 at 1.0 km. Given all the above, we fixed a pollen depolarization ratio of $\delta_{pol} = 0.40$.

To assess the impact of the uncertainty of the assumed pollen depolarization ratio, δ_{pol}, on the uncertainty of the contribution ratio of the pollen to the total particle depolarization, CR_{pol}, we consider an error $\Delta\delta_{pol}$ in the pollen depolarization ratio and write:

$$CR_{pol}(z) + \Delta CR_{pol}(z) = \frac{\delta^{P}(z) - \delta_{no-pol}}{1+\delta^{p}(z)} \frac{1+\delta_{pol}+\Delta\delta_{pol}}{\delta_{pol}+\Delta\delta_{pol}-\delta_{no-pol}}, \qquad (9)$$

from which the relative error in CR_{pol}, $\varepsilon_{rCR_{pol}} = \frac{\Delta CR_{pol}}{CR_{pol}}$, can be found as:

$$\varepsilon_{rCR_{pol}} = -\frac{\left(1+\delta_{no-pol}\right)\Delta\delta_{pol}}{\left(1+\delta_{pol}\right)\left(\delta_{pol}-\delta_{no-pol}+\Delta\delta_{pol}\right)}. \qquad (10)$$

We have calculated $\varepsilon_{rCR_{pol}}$ for various values of the "true" pollen depolarization ratio ranging from 0.2 to 0.5, when $\delta_{no-pol} = 0.03$ and $\delta_{pol} = 0.4$ is assumed. In the range $-0.1 < \Delta\delta_{pol} < +0.1$ (i.e. 0.3 < "true" pollen depolarization ratio< 0.5) the contribution ratio error is limited to ± 20 % approximately.

The profile of the pollen backscatter coefficient retrieved with Shimizu's method (see Section 2.3) and $\left(\delta_{pol} = 0.40, \delta_{no-pol} = 0.03\right)$ has, like the profiles of δ^{p}, a general tendency to decrease with increasing height, reflecting the gradual diminution of the number of pollen as height increases. In many profiles the backscatter coefficient is higher in the first 0.5 km due to the presence of a number of pollen grains larger near the ground than in altitude.

Figure 5~~Figure 5~~ shows the daily cycle of the days of the pollination event in terms of pollen concentration (total, *Platanus* and *Pinus*), PM_{10}, and a series of column-integrated lidar-derived parameters (~~AOD,~~ AOD_{pol}, AOD_{pol} / AOD, $\overline{\delta^{V}}$ and~~,~~ $\overline{\delta^{p}}$ ~~and h_{pol}~~). The AOD (not shown) was obtained by integrating the profile of β^{p} in the whole column and multiplying the result by the lidar ratio of 50 sr used in the lidar inversion. In order to be representative of the pollen plume $\overline{\delta^{V}}$ ($\overline{\delta^{p}}$) was obtained by ~~integrating~~ averaging the profile of δ^{V} (δ^{p}) from the ground up to h_{pol}, thereby limiting the ~~integration~~ averaging to the pollen plume. Table 1~~Table 1~~ gives the daily (0 – 24 UT) and diurnal (09 – 17 UT) means of all the aforementioned parameters. It is worth commenting several aspects of the daily pollen variation first. The daily and diurnal correlation coefficients, the *r*-values, of PM_{10}, AOD, AOD_{pol}, AOD_{pol} / AOD, $\overline{\delta^{V}}$, $\overline{\delta^{p}}$ and h_{pol} with the total pollen, *Platanus* and *Pinus* concentration is given in Table 2~~Table 2~~, 3~~3~~ and 4~~4~~, respectively.

Con formato: Fuente: (Predeterminada) Times New Roman, 10 pto
Código de campo cambiado
Con formato: Fuente: (Predeterminada) Times New Roman, 10 pto
Código de campo cambiado
Con formato: Fuente: (Predeterminada) Times New Roman, 10 pto
Código de campo cambiado
Con formato: Fuente: (Predeterminada) Times New Roman, 10 pto
Con formato: Fuente: (Predeterminada) Times New Roman, 10 pto
Con formato: Fuente: (Predeterminada) Times New Roman, 10 pto
Con formato: Justificado, Sangría: Primera línea: 1,25 cm
Código de campo cambiado
Con formato: Fuente: (Predeterminada) Times New Roman, 10 pto
Con formato: Fuente: (Predeterminada) Times New Roman, 10 pto
Código de campo cambiado
Con formato ... [1]
Código de campo cambiado
Con formato ... [2]
Con formato ... [3]
Con formato: Justificado, Sangría: Primera línea: 1,25 cm
Código de campo cambiado
Con formato ... [4]
Con formato ... [5]
Código de campo cambiado
Con formato ... [6]
Con formato ... [7]
Código de campo cambiado
Con formato ... [8]
Código de campo cambiado
Con formato ... [9]
Código de campo cambiado
Con formato ... [10]
Con formato: Inglés (Estados Unidos)
Con formato: Fuente: 10 pto, Sin Negrita
Con formato: Fuente: 10 pto, Sin Negrita
Con formato: Fuente: 10 pto, Sin Negrita
Con formato: Fuente: 10 pto, Sin Negrita, Oculto
Con formato: Fuente: 10 pto, Sin Negrita
Con formato: Fuente: 10 pto, Sin Negrita, Oculto
Con formato: Fuente: 10 pto, Sin Negrita

Qualitatively, two classes of days can be distinguished: the days with no (or low) nocturnal pollen near-surface activity (27 and 29 March) and the days with nocturnal pollen activity (28, 30 and 31 March). One sees that when nocturnal pollen activity is observed, high pollen concentrations are reached during the night (> 4000 m^{-3} ~~h^{-1}~~) and that on two days (28 and 31 March) the nocturnal peaks are higher than the diurnal ones. There seems to be clear indications that the nocturnal pollen activity is linked to the surface wind speed (Figure 3~~Figure 3~~b): 1) the three nights with nocturnal pollen activity correspond to the days with the highest wind speed daily means (see Section 3) and 2) on two nights (28 and 30 March) the nocturnal pollen activity coincides with the two periods of highest wind speeds (> 6 m s^{-1}). While the total pollen concentration diurnal mean is always higher than the daily mean (Table 1~~Table 1~~), the nocturnal pollen activity is able to reverse punctually this relationship for the *Platanus* and *Pinus* concentrations. A feature common to all days is the decrease of the pollen activity between 17 UT and midnight. The hourly temporal evolution of the PM_{10} is quite constant from one day to another during all five days of the pollination event. ~~No significant differences are noticeable.~~ We note that the PM_{10} values are well below the hourly mean values averaged for the month of March by Querol et al. (2001) in Barcelona which oscillate roughly between 30 and 70 µg m^{-3} ~~h^{-1}~~. The various correlation coefficients calculated for PM_{10} do not yield to conclusive results: over the whole period (27 – 31 March) the dependence of PM_{10} and pollen concentration is rather negative (positive) on a daily (diurnal) basis, but this relationship is not systematic on a day-by-day analysis. It is important to note that the overall positive diurnal *r*-values are the result of a circumstantial dependence: the pollen number morning increase and the everyday traffic PM_{10} peak occur at the same period of the day but are not linked one to another. Finally we also want to point out that PM_{10} samplers have a cut-off aerodynamic diameter at 10 µm, which is significantly smaller than the diameter of the most abundant pollen grains observed (*Platanus* and *Pinus*), thus implying that no marked correlation should be expected between PM_{10} and pollen concentration.

We now move on to the analysis of the lidar-derived columnar parameters and their possible correlations with the near-surface pollen concentration. The daily mean AOD which varies in the range 0.14 – 0.24 (Table 1~~Table 1~~) is in the range of average values for this period of the year as reported by Sicard et al. (2011). AOD_{pol} shows a clear diurnal cycle with maxima between 12 and 15 UT. The highest value of AOD_{pol}, 0.12, is reached on 30 March at 13 UT. The daily cycle and the values found here for AOD_{pol} are similar to those of Noh et al. (2013a) in a cloud of *Pinus* and *Quercus* pollen observed in South Korea. The comparison of the plots of AOD (not shown) and AOD_{pol} in Figure 5~~Figure 5~~ clearly indicates that the everyday AOD increase usually starting after 09 UT is due to the airborne pollen. The contribution of AOD_{pol} to the AOD passes every day from values below 20 % before 09 UT to maxima ranging from 28 to 78 % reached between 11 and 15 UT. On 29 and 30 March the maxima reach 61 and 78 %, respectively, while on the three other days AOD_{pol} / AOD stays below 40 %. The former maxima are quite high and suggest a strong dispersion of the pollen grains in the atmosphere. Obviously the daily and diurnal means ranging, respectively, in 11 – 23 and 20 – 40 % (Table 1~~Table 1~~) are much lower than the hourly peaks. It is also interesting to note that on the last four days of the event the nighttime values of AOD_{pol}, although low (< 0.03), are not negligible. The daily evolutions of $\overline{\delta^V}$ and $\overline{\delta^p}$ are quantitatively very similar. Like for AOD_{pol} a clear diurnal cycle is visible everyday with maxima of 0.18

Con formato: Fuente: 10 pto, Sin Negrita

Con formato: Fuente: 10 pto, Sin Negrita

Con formato: Fuente: 10 pto, Sin Negrita

Con formato: Fuente: 10 pto, Sin Negrita

Con formato: Fuente: 10 pto, Sin Negrita

(0.33) for $\overline{\delta^V}$ ($\overline{\delta^p}$) reached on 30 March at 12 UT. The diurnal mean of $\overline{\delta^V}$ ($\overline{\delta^p}$) averaged over the whole pollination event is 0.08 (0.14). Here again the nighttime values of $\overline{\delta^V}$ ($\overline{\delta^p}$) are found non-negligible on the last four days of the event. Non-negligible nighttime values of δ^V were already observed in the time-range plots of Figure 2~~Figure 2~~. Interestingly those four days correspond to the three days previously classified as days with nocturnal pollen near-surface activity, plus 29 March that was classified as a day without nocturnal pollen activity. On 29 March the non-negligible nighttime values of AOD_{pol}, $\overline{\delta^V}$ and $\overline{\delta^p}$ coincide in time with a developed pollen plume (last plot of Figure 5~~Figure 5~~). Indeed h_{pol} reaches its maximum nighttime peak, at 0.81 km, on 29 March at 04 UT. This observation suggests that near-surface pollen release and pollen plume dispersion in the atmosphere are not necessarily time~~ly~~ correlated. The daily evolutions of h_{pol} are quite similar from one day to another. Heights below 0.81 km are found before 08 UT and maxima ranging in 1.47 – 1.78 km are usually reached between 14 – 16 UT. Over the whole event the diurnal mean pollen height is 1.24 km. The diurnal increase of h_{pol} is smoother than that of AOD_{pol}, $\overline{\delta^V}$ and $\overline{\delta^p}$. As an example, let's take δ^V for the rationale. $\overline{\delta^V}$ reaches a maximum almost systematically everyday at 12 UT. While the pollen plume keeps rising vertically between 12 and 14 – 16 UT, $\overline{\delta^V}$ decreases, evidencing a dilution effect of the atmospheric pollen: the rate of the pollen vertical distribution increase is higher than that of the release of new pollen grains, if any, in the atmosphere. Finally ~~the~~ an unusual ~~sharp decrease~~ increase of h_{pol} starts on 31 March a~~t~~fter 18 UT. It is associated with 1) a strong increase of AOD (not shown) due to high values of β^p (> 5 Mm^{-1} sr^{-1}) in the first 0.5 km (see Figure 2), ~~is an indication of the sudden removal of the pollen from the ABL.~~ 2) a decrease of $\overline{\delta^V}$ and $\overline{\delta^p}$, 3) values of δ^V and δ^p below 0.5 km close to the local, background values, 3) an increase of RH (see Figure 3b) but 4) with no significant variation of the near-surface PM_{10} level. All in all these results suggest a slow dilution of the pollen within the ABL (> 0.5 km) accompanied by a possible hygroscopic growth of lofted particles, probably from local origin, below 0.5 km.

~~The fact that it is associated to a strong increase of the AOD but to any increase of the near-surface PM_{10} level suggests that the new non-depolarizing aerosol plume seen in Figure 2 with high values of β^p (> 5 Mm^{-1} sr^{-1}) and confined in the first 0.5 km is not from local origin.~~

We have calculated the correlation coefficients between the near-surface pollen concentration (total, *Platanus* and *Pinus*) and the columnar properties discussed above in this Section (Table 2~~Table 2~~, 3~~3~~ and 4~~4~~). For each parameter the highest, positive *r*-values have been colored in red. The highest daily (0 – 24 UT) *r*-values of the total pollen are on 27 March. Excepting the PM_{10} parameter the same occurs for *Pinus*, whereas for *Platanus* most of the highest *r*-values are found on 29 March. Although *Pinus* is found in lesser amounts than *Platanus*, it seems to influence strongly the total pollen columnar properties. The highest diurnal (9 – 17 UT) values are found in majority on 29 March for the total pollen and *Platanus* and on 31 March for *Pinus*. This time, during the strong diurnal pollen release, the total pollen columnar properties seem to be driven by the ones of *Platanus*.

Con formato: Fuente: 10 pto, Sin Negrita
Con formato: Fuente: 10 pto, Sin Negrita
Con formato: Sin Resaltar
Con formato: Sin Resaltar
Con formato: Sin Resaltar
Código de campo cambiado
Con formato: Sin Resaltar
Con formato: Sin Resaltar
Con formato: Sin Resaltar
Con formato: Sin Resaltar
Con formato: Sin Resaltar
Código de campo cambiado
Con formato: Sin Resaltar
Con formato: Sin Resaltar
Código de campo cambiado
Código de campo cambiado
Con formato: Sin Resaltar
Con formato: Sin Resaltar
Código de campo cambiado
Código de campo cambiado
Código de campo cambiado
Con formato: Fuente: 10 pto, Sin Negrita
Con formato: Sin Resaltar
Con formato: Sin Resaltar
Con formato: Sin Resaltar
Con formato: Sin Resaltar
Con formato: Inglés (Reino Unido)
Con formato: Fuente: 10 pto, Sin Negrita
Con formato: Fuente: 10 pto, Sin Negrita, Oculto
Con formato: Fuente: 10 pto, Sin Negrita
Con formato: Fuente: 10 pto, Sin Negrita, Oculto
Con formato: Fuente: 10 pto, Sin Negrita

For each day, the highest, positive *r*-values have been stressed in bold font. Independently of the pollen type $\overline{\delta^p}$ appears clearly to be the parameter with the highest daily *r*-values. In particular for the total pollen and *Platanus* the daily *r*-values range between 0.~~39~~ 52 and 0.81 on the first three days and between 0.12 and 0.26 ~~,~~ ~~leaving apart 30 March~~on the last two. Concerning the diurnal *r*-values, the results are not so clear: $\overline{\delta^p}$ still appears as the parameter with the highest *r*-values for *Platanus*, but no parameter clearly stands out for the total pollen and *Pinus*.

In the concern to find a possible proxy of the pollen (be it total, *Platanus* or *Pinus*) near-surface concentration with some columnar parameter easily measurable by remote sensing instrument, we examine the correlation between pollen concentration and AOD. The AOD is a columnar parameter which is relatively easily measurable, e.g. with a sun-photometer, and which can be retrieved with a relatively high accuracy. For example in the AERONET (Aerosol Robotic Network; http://aeronet.gsfc.nasa.gov/) worldwide network of sun/sky-photometers, the accuracy is ± 0.02 (Eck et al., 1999). Table 2~~Table 2~~, 3~~3~~ and 4~~4~~ show that the *r*-values of the AOD parameter, although in majority negative, can frequently change sign and reach values close to zero. The AOD is therefore not an appropriate proxy for the pollen near-surface concentration. It is interesting to note, en passant, that AOD_{pol} *r*-values are not much better and that AOD_{pol} would not be a good proxy either. This result emphasizes again that near-surface pollen release and columnar pollen dispersion are not time~~ly~~ correlated. The correlation between pollen concentration and δ^V is also investigated because δ^V is a lidar product relatively simple to retrieve since it does not require post-acquisition processing. In the case of the MPL system used in this study, δ^V is obtained by a very simple operation with the two collected powers (see Eq. (3)~~(3)~~). Although $\overline{\delta^V}$ *r*-values are usually a little lower than $\overline{\delta^p}$ values, the values indicate globally a rather positive correlation between $\overline{\delta^V}$ and the pollen concentration. To investigate further the pros and contras of using $\overline{\delta^V}$ instead of $\overline{\delta^p}$, the retrieval of which is much less straight-forward than the retrieval of $\overline{\delta^V}$, we present in Figure 6~~Figure 6~~ the scatter plots of the daily (0 – 24 UT) values of pollen concentration vs. $\overline{\delta^V}$ and $\overline{\delta^p}$. In this figure the positive slope of the red linear regression line is a clear indicator of the positive correlation between $\overline{\delta^V}$ / $\overline{\delta^p}$ and the pollen concentration. Over the whole event the $\overline{\delta^p}$ ($\overline{\delta^V}$; $\overline{\delta^V} - \overline{\delta^p}$) *r*-values are 0.41 (0.34; -0.07) for total pollen, 0.36 (0.28; -0.08) for *Platanus* and 0.46 (0.42; -0.04) for *Pinus*. Thus overall the $\overline{\delta^V}$ *r*-values are between -0.08 and -0.04 smaller than the $\overline{\delta^p}$ ones. The highest $\overline{\delta^V}$ and $\overline{\delta^p}$ *r*-values are reached for *Pinus* ($0.09 < \overline{\delta^V}\ r-values < 0.70$ and $0.25 < \overline{\delta^p}\ r-values < 0.68$), while the lowest *r*-values are reached for *Platanus* ($0.02 < \overline{\delta^V}\ r-values < 0.68$ and $0.12 < \overline{\delta^p}\ r-values < 0.70$). One also sees that the days previously classified as days with nocturnal pollen near-surface activity (28, 30 and 31 March) have the lowest *r*-values. This is mostly due to the points with high concentration and low depolarization ratios visible above the linear regression line, reflecting the nighttime situation of high pollen release without vertical

Con formato: Fuente: 10 pto, Sin Negrita

Con formato: Fuente: 10 pto, Sin Negrita, Oculto

Con formato: Fuente: 10 pto, Sin Negrita, Revisar la ortografía y la gramática

Con formato: Fuente: 10 pto, Sin Negrita, Oculto

Con formato: Fuente: 10 pto, Sin Negrita, Revisar la ortografía y la gramática

Con formato: Fuente: 10 pto, Sin Negrita

dispersion. For the days classified as days without nocturnal pollen activity the difference between $\overline{\delta^V}$ and $\overline{\delta^p}$ *r*-values are in general smaller than 0.04, so that it becomes nearly equivalent to use $\overline{\delta^V}$ instead of $\overline{\delta^p}$. For these days the highest $\overline{\delta^V}$ *r*-values are reached for the total pollen. Let's note that the total pollen release and dispersion is especially well correlated on 27 March ($\overline{\delta^V}$ and $\overline{\delta^p}$ *r*-values are equal to 0.81). All in all these results suggest that:

- In all conditions:
  - Differences between $\overline{\delta^V}$ and $\overline{\delta^p}$ *r*-values range between 0.08 and 0.04.
  - $\overline{\delta^V}$ seems to be a proxy better for *Pinus* and the total pollen concentration than for *Platanus* concentration.
- Without nocturnal pollen near-surface activity:
  - $\overline{\delta^V}$ and $\overline{\delta^p}$ are nearly equivalent (*r*-values differences smaller than 0.04).
  - $\overline{\delta^V}$ seems to be an appropriate proxy for the total pollen concentration.

It is important to recall that these conclusions have to be taken in a general sense, and that, depending on the meteorological conditions, there may be cases for which these statements do not apply. In the following Section we seek the possible reasons which could explain the aforementioned correlations between pollen near-surface concentration and columnar depolarization ratios.

5. Influence of the solar radiation on the pollen vertical transport in the atmosphere

For the pollen to be dispersed in the atmosphere, vertical transport is needed. According to Mandrioli et al. (1984) the main mechanism driving the vertical movement of atmospheric particles is the atmospheric turbulence. In the ABL atmospheric turbulences result from the vertical movement of air masses due to the heating and cooling of the ground by the sun and to the flow of air (wind) over the ground. At the end of Section 3 we showed that the pollen AOD did not present a systematic dependence upon wind speed, because of the low wind speeds (usually lower than 3 m s^{-1}) detected during the pollination event. Thus we examine the possible influence of solar radiations on the vertical transport of pollen thanks to MPL co-located pyranometer solar flux measurements performed at the Barcelona SolRad-Net (Solar Radiation Network, http://solrad-net.gsfc.nasa.gov/) site. The pyranometer is a Kipp and Zonen CMP21 sensor that provides every two minutes a measurement of the total solar flux in the range 0.3 – 2.8 µm. We used SolRad-Net level 1.5 data which have been cleared as free of any operational problems. The solar flux (also called solar irradiance) measured at ground level is the power per unit area produced by the sun in the form of electromagnetic radiation measured at the Earth's surface after atmospheric absorption and scattering.

Figure 7~~Figure 7~~ shows the solar fluxes as a function of time for all five days of the pollination event. On 29 and 30 March clouds alter significantly the diurnal pattern of the solar radiation received at ground level. We have checked on the profiles of the MPL the presence of clouds and their altitude on the three clear-sky days~~.~~ ~~On 29 March medium- and high-level clouds were present along the day in the range of 5 to 12 km, while on 30 March high-altitude clouds between 9 and 13 km were present along the day. The most part of the days of 27 and 28 March were free of clouds.~~ -On 27 March high-level clouds in the range 9 – 12 km were present until 09:30 UT, while on 28 March clouds in the range 8 – 10 km were present until 10 UT and again after 17 UT. On 31 March the sky was totally free of clouds with the exception of clouds forming in the ABL from 17 UT onwards. The possible influence of the solar radiations on the vertical transport of pollen is examined with the clear-sky days of 27, 28 and 31 March. In the first row of Figure 8~~Figure 8~~ we represent all together the solar fluxes, $\overline{\delta^V}$, ~~and~~ $\overline{\delta^p}$ and AOD_{pol} as a function of time. Everyday a diurnal pattern is clearly visible on all curves with an increase in the morning and a decrease in the afternoon. On 27 March the temporal evolution of $\overline{\delta^V}$ and $\overline{\delta^p}$ seems to follow especially well the pattern of the solar flux. In all three cases a time delay is observed between the diurnal evolution of the solar fluxes and the depolarization ratios and of the solar fluxes and AOD_{pol}. As one could intuitively expect, the pollen vertical transport pattern, triggered by the turbulences caused by the heating/cooling of the ground, should follow with a given time delay (i.e. start after) that of the solar flux. The top plots of Figure 8 clearly show that the temporal evolution of AOD_{pol} is always delayed w.r.t. the solar fluxes. In order to quantify that time delay, *t*, for each day ~~and~~ , for each of the two depolarization ratios and for AOD_{pol}, we have searched the value of *t* that maximizes the correlation coefficient defined as:

$$r(\mathrm{t}) = r\left(F(\mathrm{x}), \delta(\mathrm{x}-\mathrm{t})\right) \qquad (11~~9~~)$$

where F is the solar flux and δ either $\overline{\delta^V}$, ~~or~~ $\overline{\delta^p}$ or AOD_{pol}. The optimized value of *t* that maximizes the correlation coefficient is called t_{opt}. The second ~~and~~, third and fourth rows of Figure 8~~Figure 8~~ present the scatter plots of the solar flux vs. $\overline{\delta^V}$, ~~and~~ $\overline{\delta^p}$ and AOD_{pol}, respectively. We have represented the scatter plots without time delay (red colour, $r(t=0)$) and the scatter plots with a time delay equal to t_{opt} (blue colour, $r(t=t_{opt})$). ~~In the first row of Figure 8 we have indicated with an arrow the direction of translation of the $\overline{\delta^V}$ / $\overline{\delta^p}$ curves that t_{opt} implies.~~ The $\overline{\delta^V}$ *r*-values without time delay are in the range 0.~~70~~49 – 0.86, which already indicates a good correlation between the solar flux and $\overline{\delta^V}$. The *r*-values for $t=t_{opt}$ are significantly better as they range from 0.~~85~~90 to 0.~~8~~95. On 27 and 31 March t_{opt} = -1 and -2 hours, respectively, which indicates that the diurnal pattern of $\overline{\delta^V}$ follows that of the solar flux delayed ~~approximately~~ 1 and 2 hours. On 28 March t_{opt} = +1 hour which indicates that the diurnal pattern of $\overline{\delta^V}$ is ahead of that of the solar flux approximately 1 hour. Let's recall that 28 March is one of the days with nocturnal pollen near-surface activity and with the highest wind speeds. The maximum observed at 09 UT is due to a low layer of pollen (< 0.5 km) with relatively high values of $\overline{\delta^V}$ (see Figure 3~~Figure 3~~b). As far as $\overline{\delta^p}$ is concerned, the *r*-values without time delay (

Con formato: Fuente: 10 pto, Sin Negrita

Con formato: Fuente: 10 pto, Sin Negrita

Con formato: Subíndice

Con formato: Subíndice

Código de campo cambiado

Con formato: Fuente: 10 pto, Sin Negrita

Con formato: Subíndice

Con formato: Subíndice

Con formato: Subíndice

Con formato: Fuente: 10 pto, Sin Negrita

Con formato: Subíndice

Con formato: Fuente: 10 pto, Sin Negrita

$0.45 < \overline{\delta^p}\ r(t=0) - values < 0.89$) are also significantly improved when an optimized time delay is applied ($0.80 < \overline{\delta^p}\ r(t=t_{opt}) - values < 0.91$). The optimized value of *t* for $\overline{\delta^p}$ The t_{opt} are the same than for $\overline{\delta^v}$ (except on 27 March when t_{opt} = 0 for $\overline{\delta^p}$)values vary from 0 to +1 hour between those of $\overline{\delta^v}$ and $\overline{\delta^p}$. After the optimized time delay is applied, $\overline{\delta^v}$ *r*-values are all greater or equal to the $\overline{\delta^p}$ *r*-values. Differences vary between +0.030 and +0.08. These findings indicate that $\overline{\delta^v}$ is better correlated to the solar flux than $\overline{\delta^p}$ is. This happens probably because δ^V retrieval is much more straightforward than δ^p retrieval and thus its uncertainty is smaller., which makes sense since both $\overline{\delta^v}$ and the solar fluxes depend on the molecules and the particles, while $\overline{\delta^p}$ depends only on the particles. For AOD_{pol}, the *r*-values without time delay ($0.37 < AOD_{pol}\ r(t=0) - values < 0.84$) are lower than the ones of the depolarization ratios, but they become higher when an optimized time delay is applied ($0.91 < AOD_{pol}\ r(t=t_{opt}) - values < 0.98$). The optimized time delays are all negative, as foreseen from the top plot of Figure 8, and vary between -1 and -3 hours. Among the three parameters studied ($\overline{\delta^V}$, $\overline{\delta^p}$ and AOD_{pol}), AOD_{pol} presents the highest correlation with the solar radiation reaching the ground. The most probable explanation of this finding is that AOD_{pol} is a measure intrinsic to pollen while $\overline{\delta^V}$ and $\overline{\delta^p}$ depend partly on the mixing of pollen with local aerosols.

6. Conclusion

For the first time near-surface and columnar measurements of airborne pollen have been performed continuously at a temporal resolution of one hour during a 5-day pollination event in a large European city. At the peak of the event 2830 pollen and fungal spore grains were counted per cubic meter per day. *Platanus* and *Pinus* pollen types represented together more than 80 % of the total concentration. Hourly concentration maxima of 4700 and 1200 m^{-3} h^{-1} were found for *Platanus* and *Pinus*, respectively. Except on one day, the total pollen concentration at ground level followed a clear diurnal cycle and was correlated positively with temperature (r = 0.95) and wind speed (r = 0.82) but negatively with relative humidity (r = -0.18). These results indicate a strong dependence of pollen release upon the meteorological conditions, especially temperature and wind speed. As far as pollen AOD is concerned, its peaks were systematically associated with minima of relative humidity and maxima of temperature but they did not present a systematic dependence upon wind speed.

The pollen AOD showed a clear diurnal cycle with maxima between 12 and 15 UT. The diurnal (9 – 17 UT) mean of AOD_{pol} was 0.05 over the whole event and represented 29 % of the total AOD. However peaks of AOD_{pol} and AOD_{pol} / AOD of, respectively, 0.12 and 78 % were found on the hourly data. The diurnal mean

Código de campo cambiado
Código de campo cambiado
Con formato: Fuente: Cursiva
Con formato: Fuente: Cursiva, Subíndice
Código de campo cambiado
Código de campo cambiado
Código de campo cambiado
Con formato: Resaltar
Código de campo cambiado
Con formato: Resaltar
Código de campo cambiado
Con formato: Resaltar
Con formato: Subíndice
Código de campo cambiado
Código de campo cambiado
Código de campo cambiado
Con formato: Fuente: 10 pto, Sin Negrita
Código de campo cambiado
Código de campo cambiado
Con formato: Subíndice
Con formato: Subíndice
Con formato: Subíndice
Código de campo cambiado
Código de campo cambiado

volume and particle depolarization ratios in the pollen plume were 0.08 and 0.14, with hourly maxima of 0.18 and 0.33, respectively. The diurnal height of the pollen plume was found at 1.24 km on average with maxima varying in the range 1.47 – 1.78 km.

We have investigated the possible correlations between pollen near-surface concentration and columnar properties. Between concentration and AOD (be it total or pollen AOD) the correlation was rather poor which emphasizes that near-surface pollen release and columnar pollen dispersion are not timely correlated. $\overline{\delta^V}$ and $\overline{\delta^p}$ were positively correlated with the total pollen concentration. The daily mean $\overline{\delta^V}$ and $\overline{\delta^p}$ *r*-values were, respectively, 0.34 and 0.41, with maxima of 0.81 reached on the first day of the event for both parameters. If we remove the days with nocturnal pollen near-surface activity, $\overline{\delta^V}$ and $\overline{\delta^p}$ *r*-values were greater than 0.68 and their difference smaller than 0.04. $\overline{\delta^V}$, and a fortiori $\overline{\delta^p}$, appeared to be an appropriate proxy for the total pollen concentration, especially when no pollen nocturnal activity is recorded.

The possible influence of solar radiations, which cause the atmospheric turbulences responsible for the aerosol vertical motion, on the vertical transport of pollen was examined by means of $\overline{\delta^V}$, $\overline{\delta^p}$, AOD_{pol} and solar fluxes measured during the three clear-sky days of the pollination event. Correlation coefficients better than 0.7049 (0.495; 0.37) were obtained for $\overline{\delta^V}$ ($\overline{\delta^p}$; AOD_{pol}) vs. solar flux. In all cases we could find a time delay between the pattern of the pollen vertical transport and the one of the solar flux that could maximize the *r*-values. After the optimized time delay was applied, correlation coefficients better than 0.85 90 (0.7780; 0.91) were obtained for $\overline{\delta^V}$ ($\overline{\delta^p}$; AOD_{pol}) vs. solar flux. This study demonstrates that, in the absence of other depolarizing particles, the volume depolarization ratio is an excellent tool to track airborne pollen grains. On the one hand it is relatively well correlated with the pollen near-surface concentration which quantifies the pollen release; and on the other hand it is very well correlated with the solar fluxes on which the pollen vertical dispersion depends.

In our opinion this work puts forward two potential perspectives. First, relatively simple polarization-sensitive lidar systems (with at least two channels) able to produce continuously profiles of the volume depolarization ratio are very attractive tools for modellers to validate their pollen concentration forecasting models and/or perform data assimilation. The question was raised for PM_{10} concentration by Wang et al. (2013). Second, the fact that large grains of pollen (of diameter ranging roughly in 20 – 70 µm) are capable of producing AOD of 0.12 raises the question of their effect in terms of radiative forcing. Otto et al. (2011) demonstrated that large mineral dust particles with a diameter of 50 µm produced a radiative forcing at the surface almost four times greater than the one produced by particles with a diameter of 5 µm. Large pollen grains may behave the same. Further research on that subject is definitely necessary.

Con formato: Subíndice

Con formato: Subíndice

Con formato: Subíndice

Acknowledgments

Lidar data analysis were supported by the ACTRIS (Aerosols, Clouds, and Trace Gases Research Infrastructure Network) Research Infrastructure Project funded by the European Union's Horizon 2020 research and innovation programme under grant agreement n. 654169 and previously under grant agreement n. 262254 in the 7th Framework Programme (FP7/2007-2013); by the Spanish Ministry of Economy and Competitivity (projects TEC2012-34575 and TEC2015-63832-P) and of Science and Innovation (project UNPC10-4E-442) and EFRD (European Fund for Regional Development); by the Department of Economy and Knowledge of the Catalan autonomous government (grant 2014 SGR 583). The authors also thank Xavier Lleberia and Marc Rico from the Agència de Salut Pública de l'Ajuntament de Barcelona for providing the PM_{10} measurements, and the Facultad de Física of the Universitat de Barcelona for providing the meteorological measurements. Andrés Alastuey and Cristina Reche from the Instituto de Diagnóstico Ambiental y Estudios del Agua / Consejo Superior de Investigaciones Científicas (IDÆA / CSIC) are thanked for their useful advice about the PM_{10} measurements.

References

Alba, F., Díaz de la Guardia, C., and Comtois, P.: The effect of meteorological parameters on diurnal patterns of airborne olive pollen concentration, Grana, 39, 200-208, 2000.

Alba, F., De La Guardia, C. D., and Comtois, P.: The effect of meteorological parameters on diurnal patterns of airborne olive pollen concentration, Grana, 39, 200–208, 2000.

Bartková- Ščevková, J.: The influence of temperature, relative humidity and rainfall on the occurrence of pollen allergens (Betula, Poaceae, Ambrosia artemisiifolia) in the atmosphere of Bratislava (Slovakia), Int. J. Biometeorol., 48, 1–5, 2003.

Behrendt, A. and Nakamura, T.: Calculation of the calibration constant of polarization lidar and its dependency on atmospheric temperature, Optics Express, 10, 805–817, 2002.

Belmonte, J., Canela, M., Guàrdia, R., Guàrdia, R.A., Sbai, L., Vendrell, M., Cariñanos, P., Díaz de la Guardia, C., Dopazo, A., Fernández, D., Gutiérrez, M., and Trigo, M.M.: Aerobiological dynamics of the Cupressaceae pollen in Spain, 1992-98, Polen, 10, 27-38, 1999.

Belmonte, J., De Linares, C., Fernández-Llamazares, A., Díaz de la Guardia, C., Cariñanos, P, Alonso-Perez, S, Cuevas, E., Maya, J., Fernández, S., Silva, I., and Tormo, R.: Airborne *Pinus* pollen in Spain: pollination patterns and trends of the annual indexes and the peak dates, Alergologia Immunologia, 9 (2-3), 166, 2012.

Belmonte, J., and Roure, J.M.: Characteristics of the aeropollen dynamics at several localities in Spain, Grana, 30, 361-372, 1991.

Boers, R., Spinhirne, J. D., and Hart, W. D.: Lidar Observations of the Fine-Scale Variability of Marine Stratocumulus Clouds, J. Appl. Meteorol., 27, 797–810, 1988.

Burch, M., and Levetin, E.: Effects of meteorological conditions on spore plumes. International Journal of Biometeorology, 46, 107–117, 2002.

Burge, H.A., and Rogers, C.A.: Outdoor allergens, Environ. Health Perspect., 108, 653–659, 2000.

Campbell, J. R., Hlavka, D.L., Welton, E. J., Flynn, C. J., Turner, D. D., Spinhirne, J. D., Scott, V. S., and Hwang, I. H.: Full-time, eye-safe cloud and aerosol lidar observation at Atmospheric Radiation Measurement Program sites: instruments and data processing, J. Atmos. Ocean. Tech., 19, 431-442, 2002.

Cao, X., Roy, G., and Bernier, R.: Lidar polarization discrimination of bioaerosols, Opt. Eng., 49(11), 116201, 1-12, 2010.

Cecchi, L.: From pollen count to pollen potency: the molecular era of aerobiology, Eur. Respir. J., 42, 898-900, doi: 10.1183/09031936.00096413, 2013.

Dahl, A., Galán, C., Hajkova, L., Pauling, A., Sikoparija, B., Smith, M., and Vokou, D.: The Onset, Course and Intensity of the Pollen Season. In Sofiev, M. and Bergmann, K-Ch. (Eds.), Allergenic Pollen. A review of the Production, Release, Distribution and Health Impacts, 29-70. ISBN 978-94-007-4881-1-3, doi: 10.1007/978-94-007-4881-1, Springer, 2013.

De Linares, C., Postigo, I., Belmonte, J., Canela, M., and Martínez, J.: Optimization of the measurement of outdoor airborne allergens using a protein microarrays platform, Aerobiologia, 30, 217-227, doi: 10.1007/s10453-013-9322-2, 2014.

Denning, D.W., O'Driscoll, B.R., Hogaboam, C.M., Bowyer, P., and Niven, R.M.: The link between fungi and severe asthma: a summary of the evidence, Eur. Respir. J., 27, 615–626, 2006.

Díaz de la Guardia, C.,Sabariego, S., Alba, F.,Ruiz, L., García Mozo, H., Toro Gil, F.J., Valencia, R., Rodríguez Rajo, F.J., Guàrdia, A., and Cervigón, P.: Aeropalynological study of the genus *Platanus* L. in the Iberian Peninsula, Polen, 10, 89-97, 1999.

Eck, T. F., Holben, B. N., Reid, J. S., Dubovik, O. Kinne, S., Smirnov, A., O'Neill, N. T., and Slutsker, I.: The wavelength dependence of the optical depth of biomass burning, urban and desert dust aerosols, J. Geophys. Res., 104, 31333–31349, 1999.

Fernald, F. G.: Analysis of atmospheric lidar observations: some comments, Appl. Opt., 23, 652–653, 1984.

Flynn, C. J., Mendoza, A., Zheng, Y., and Mathur, S.: Novel polarization-sensitive micropulse lidar measurement technique, Optics Express, 15, 6, 2785-2790, 2007.

Freudenthaler, V., Esselborn, M., Wiegner, M., Heese, B., Tesche, M., Ansmann, A., Muller, D., Althausen, D., Wirth, M., Fix, A., Ehret, G., Knippertz, P., Toledano, C., Gasteiger, J., Garhammar, M., and Seefeldner, M.: Depolarizationratio profiling at several wavelengths in pure Saharan dust during SAMUM 2006, Tellus B, 61, 165–179, doi:10.1111/j.1600-0889.2008.00396.x, 2009.

Gabarra, E., Belmonte, J., and Canela, M.: Aerobiological behaviour of *Platanus* L. pollen in Catalonia (North-East Spain), Aerobiologia, 18, 185-193, 2002.

Galán Soldevilla, C., Cariñanos González, P., Alcázar Teno, P., and Domínguez Vilches, E.: Manual de Calidad y Gestión de la Red Española de Aerobiología, Servicio de Publicaciones, Universidad de Córdoba, 2007.

Gimmestad, G. G.: Reexamination of depolarization in lidar measurements, Appl. Opt., 47, 21, 3795-3802, 2008.

Grinn-Gofrón, A., and Strzelczak, A.: Artificial neural network models of relationships between *Cladosporium* spores and meteorological factors in Szczecin (Poland), Grana, 47, 305–315, 2008.

Hart, M., Wentworth, J., and Bailey, J.: The effects of trap height and weather variables on recorded pollen concentration at Leicester, Grana, 33, 100–103, 1994.

Hirst, J.M.: An automatic volumetric spore trap, Ann. Appl. Biol., 39, 257-265, 1952.

Huang, Z., Huang, J., Bi, J., Wang, G., Wang, W., Fu, Q., Li, Z., Tsay, S.-C., and Shi, J.: Dust aerosol vertical structure measurements using three MPL lidars during 2008 China-U.S. joint dust field experiment, J. Geophys. Res., 115, D00K15, doi:10.1029/2009JD013273, 2010.

Infante, F., Castro, A., Domínguez, E., Guárdia, A., Méndez, J., Sabariego, S., and Vega, A.: A comparative study of the incidence of *Cladosporium* conidia in the atmosphere of five Spanish cities, Polen, 10, 15-23, 1999.

Jato, M., Rodríguez, F., and Seijo, M.: Pinus pollen in the atmosphere of Vigo and its relationship to meteorological factors, Int. J. Biometeorol., 43, 147–153, 2000.

Karatzas, K.D., Riga, M., and Smith, M.: Presentation and Dissemination of Pollen Information. In Sofiev, M. and Bergmann K-Ch. (Eds.), Allergenic Pollen. A review of the Production, Release, Distribution and Health Impacts, 217-247. ISBN 978-94-007-4881-1-7, doi: 10.1007/978-94-007-4881-1. Springer, 2013.

Klett, J. D.: Lidar inversion with variable backscatter/extinction ratios, Appl. Opt. 24, 1638–1643, 1985.

Lacey, J.: The aerobiology of conidial fungi, Biology of Conidial Fungi, 1, 373–416, 1981.

Landulfo, E., Papayannis, A., Artaxo, P., Castanho, A. D. A., de Freitas, A. Z., Souza, R. F., Vieira Junior, N. D., Jorge, M. P. M. P., Sánchez-Ccoyllo, O. R., and Moreira, D. S.: Synergetic measurements of aerosols over São Paulo, Brazil using LIDAR, sunphotometer and satellite data during the dry season, Atmos. Chem. Phys., 3, 1523–1539, doi:10.5194/acp-3-1523-2003, 2003.

Latorre, F., and Caccavari, M. A.: Airborne pollen patterns in Mar del Plata atmosphere (Argentina) and its relationship with meteorological conditions, Aerobiologia, 25, 297-312, doi: 10.1007/s10453-009-9134-6, 2009.

Lopez, M., and Salvaggio, J.E.: Mold-sensitive asthma, Clin. Rev. Allergy, 3, 183–196, 1985.

Mandrioli, P., Negrini, M.G., Cesari, G., and Morgan, G.: Evidence for long range transport of biological and anthropogenic aerosol particles in the atmosphere, Grana 23, 43-53, 1984.

McCartney, H. A.: Dispersal of spores and pollen from crops, Grana, 33:2, 76-80, doi: 10.1080/00173139409427835, 1994.

Melfi, S. H., Spinhirne, J. D., Chou, S. H., and Palm, S. P.: Lidar Observation of the Vertically Organized Convection in the Planetary Boundary Layer Over the Ocean, J. Clim. Appl. Meteorol., 24, 806–821, 1985.

Noh, Y. M., Müller, D., Lee, H. L., and Choi, T. J.: Influence of biogenic pollen on optical properties of atmospheric aerosols observed by lidar over Gwangju, South Korea, Atmos. Environ., 69, 139-147, doi: dx.doi.org/10.1016/j.atmosenv.2012.12.018, 2013a.

Noh, Y. M., Lee, H., Müller, D., Lee, K., Shin, D., Shin, S., Choi, T. J., Choi, Y. J., and Kim, K. R.: Investigation of the diurnal pattern of the vertical distribution of pollen in the lower troposphere using LIDAR, Atmos. Chem. Phys., 13, 7619 – 7629, doi:10.5194/acp-13-7619-2013, 2013b.

Otto, S., Trautmann, T., and Wendisch, M.: On realistic size equivalence and shape of spheroidal Saharan mineral dust particles applied in solar and thermal radiative transfer calculations, Atmos. Chem. Phys. 11, 4469–4490, doi:10.5194/acp-11-4469-2011, 2011.

Pakpour, S., Li, D.W., and Klironomos, J.: Relationships of fungal spore concentrations in the air and meteorological factors, Fungal Ecology, 13, 130-134, 2015.

Puiggròs, A., Muñoz-Cano, R., Roger Reig, A., Raga, E., Belmonte, J., and Valero, A.: Prevalence of Sensitization to Pollen From Trees Planted in Barcelona City, J Investig Allergol Clin Immunol, 25(2), 133-162, 2015.

Querol, X., Alastuey, A., Rodríguez, S., Plana, F., Ruiz, C. R., Cots, N., Massagué, G., and Puig, O.: PM10 and PM2.5 source apportionment in the Barcelona metropolitan area, Catalonia, Spain. Atmos. Environ., 35, 6407–6419, 2001.

Raynor, G. S., Ogden, E. C., and Hayes, J. V.: Variation in ragweed pollen concentration to a height of 108 meters, J. Allergy Clinical Immun., 51, 199–207, 1973.

Reba, M. N. M., Rocadenbosch, F., Sicard, M., Kumar, D., and Tomás, S.: On the lidar ratio estimation from the synergy between AERONET sun-photometer data and elastic lidar inversion, Proc. of the 25th International Laser Radar Conference, vol. 2, ISBN 978-5-94458-109-9, Saint-Petersburg (Rusia), 5–9 July 2010, 1102–1105, 2010.

Roy, G., Cao, X., and Bernier, R.: On the information content of linear and circular depolarization signatures of bioaerosols, Proc. of SPIE Chemical, Biological, Radiological, Nuclear, and Explosives (CBRNE) Sensing XII, Fountain, A. W., and Gardner, P. J. (Eds), Proc. of SPIE Vol. 8018, 801807,· 1-8, doi: 10.1117/12.883713, 2011.

Sasano, Y. and Nakane, H.: Significance of the extinction/backscatter ratio and the boundary value term in the solution for the two-component lidar equation, Appl. Opt. 23, 11–13, 1984.

Sassen, K.: Boreal tree pollen sensed by polarization lidar: depolarizing biogenic chaff, Geophys. Res. Lett., 35, L18810, doi: 10.1029/2008GL035085, 2008.

Scheifinger, H., Belmonte, J., Buters, J., Celenk, S., Damialis, A., Dechamp, Ch., García-Mozo, H., Gehrig, R., Grewling, L., Halley, J.M., Hogda, K-A., Jäger, S., Karatzas, K., Karlsen, S-R., Koch, E., Pauling, A., Peel, R., Sikoparija, B., Smith, M., Galán-Soldevilla, C., Thibaudon, M., Vokou, D., and de Weger, L.A.: Monitoring, Modeling and forecasting of the Pollen Season. In Sofiev, M. and Bergmann K-Ch. (Eds.), Allergenic Pollen. A review of the Production, Release, Distribution and Health Impacts, 127-158, ISBN 978-94-007-4881-1-4, doi: 10.1007/978-94-007-4881-1. Springer, 2013.

Shimizu, A., Sugimoto, N., Matsui, I., Arao, K., Uno, I., Murayama, T., Kagawa, N., Aoki, K., Uchiyama, A., and Yamazaki, A.: Continuous observations of Asian dust and other aerosols by polarization lidars in China and Japan during ACE-Asia, J. Geophys. Res., 109, D19S17, doi: 10.1029/2002JD003253, 2004.

Sicard, M., Pérez, C., Rocadenbosch, F., Baldasano, J. M., and García-Vizcaino, D.: Mixed-layer depth determination in the Barcelona coastal area from regular lidar measurements: methods, results and limitations, Bound.-Lay. Meteorol., 119, 135–157, 2006.

Sicard, M., Rocadenbosch, F., Reba, M. N. M., Comerón, A., Tomás, S., García-Vízcaino, D., Batet, O., Barrios, R., Kumar, D., and Baldasano, J. M.: Seasonal variability of aerosol optical properties observed by means of a Raman lidar at an EARLINET site over Northeastern Spain, Atmos. Chem. Phys., 11, doi:10.5194/acp-11-175-2011, 2011.

Simon-Nobbe, B., Denk, U., Pöll, V., Rid, R., and Breitenbach, M.: The spectrum of fungal allergy, Int. Arch. Allergy Immunol., 145, 58-86, 2008.

Skjøth, C.A., Sikoparija, B., and Jäger, S.: Pollen sources. In Sofiev, M. and Bergmann K-Ch. (Eds.) Allergenic Pollen. A review of the Production, Release, Distribution and Health Impacts, 9-27, ISBN 978-94-007-4881-1-2, doi: 10.1007/978-94-007-4881-1, Springer, 2013.

Skjøth, C.A., Damialis, A., Belmonte, J., De Linares, C., Fernández-Rodríguez, S., Grinn-Gofroń, A., Jędryczka, M., Kasprzyk, I., Magyar, D., Myszkowska, D., Oliver, G., Páldy, A., Pashley, C. H., Rasmussen, K., Satchwell, J., Thibaudon, M., Tormo-Molina, R., Vokou, D., Ziemianin, M., and Werner, M.: Alternaria spores in the air across Europe: abundance, seasonality and relationships with climate, meteorology and local environment, Aerobiologia, doi: 10.1007/s10453-016-9426-6, 2016.

Sofiev, M., Belmonte, J., Gehrig, R., Izquierdo, R., Smith, M., Dahl, A., and Siljamo, P.: Airborne Pollen Transport. In Sofiev, M. and Bergmann K-Ch. (Eds.), Allergenic Pollen. A review of the Production, Release, Distribution and Health Impacts, 127-158, ISBN 978-94-007-4881-1-5, doi: 10.1007/978-94-007-4881-1. Springer, 2013.

Spinhirne, J. D.: Micro pulse lidar, IEEE Trans. Geosci. Remote Sens., 31, 48-55, 1993.

Sugimoto, N., Huang, Z., Nishizawa, Y., Matsui, I., and Tatarov, B.: Fluorescence from atmospheric aerosols observed with a multi-channel lidar spectrometer, Optics Express, 20 (19), doi: 10.1364/OE.20.020800, 2012.

Vázquez, L., Galán, C., and Domínguez-Vilches, E.: Influence of meteorological parameters on olea pollen concentrations in Córdoba (South-western Spain), Int. J. Biometeorol., 48, 83–90, 2003.

Wang, Y., Sartelet, K. N., Bocquet, M., and Chazette, P.: Assimilation of ground versus lidar observations for PM10 forecasting, Atmos. Chem. Phys., 13, 269–283, doi: 10.5194/acp-13-269-2013, 2013.

WHO: World Health Report 2003: A Vision for Global Health, Shaping the Future, World Health Organization, 2003.

Weikl, F., Radl, V., Munch, J.C., and Pristch, K.: Targeting allergenic fungi in agricultural environments aids the identification of major sources and potential risks for human health, Science of The Total Environment, 529, 223-230, 2015.

Wodehouse, R. P.: Pollen grains, McGraw-Hill, New York, 1935.

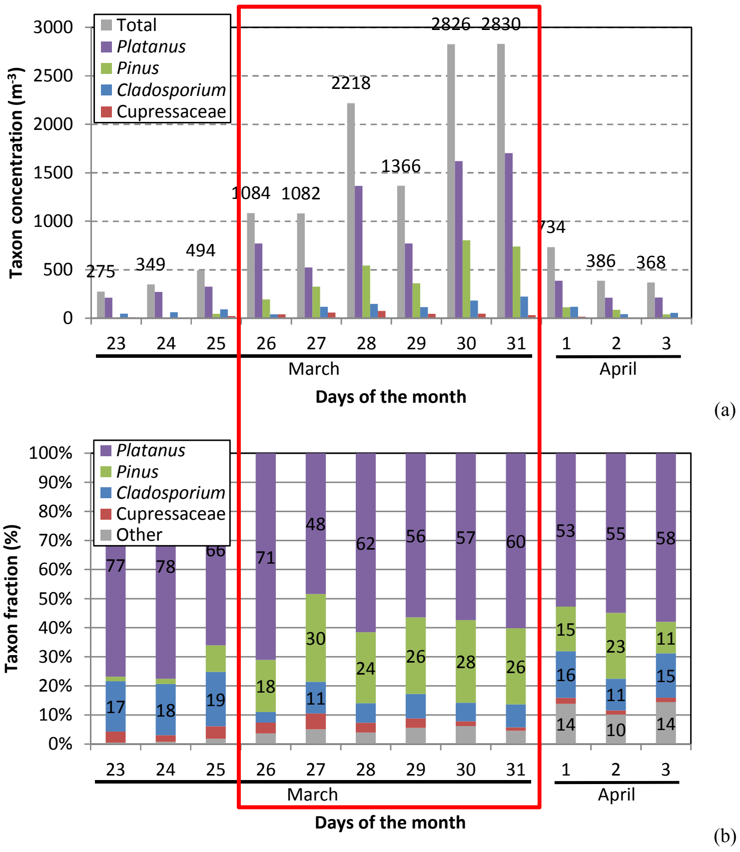

Figure 1. (a) Daily concentration of the four most abundant pollen (*Platanus*, *Pinus* and Cupressaceae) and fungal spore (*Cladosporium*) taxa and total (pollen + spore), and (b) fraction of these four taxa during the period 23 March – 3 April, 2015. The red rectangle indicates the intense pollination event. The values of the total concentrations are reported in Figure 1~~Figure 1~~a. The fractions higher than 10 % are reported in Figure 1~~Figure 1~~b.

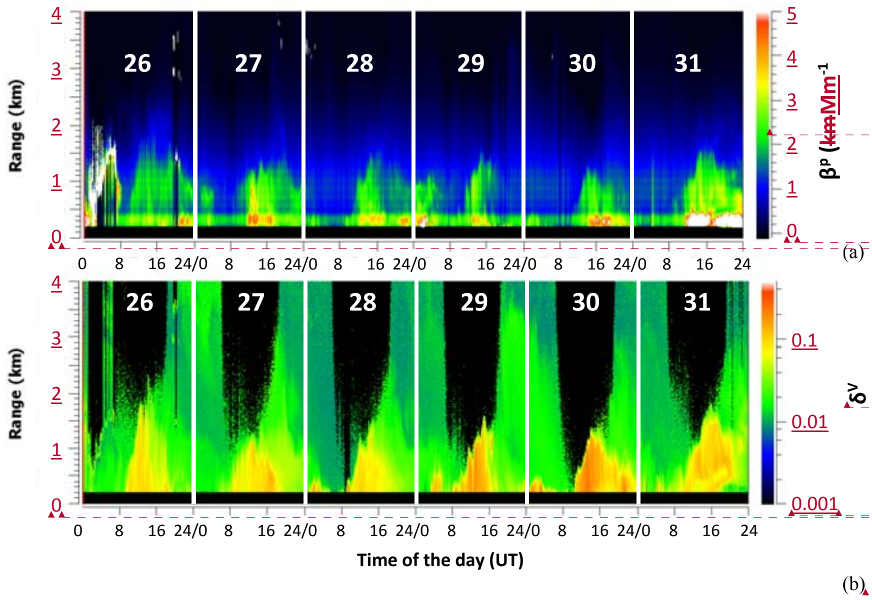

Figure 2. 5-min. resolution time-range plots of the (a) particle backscatter coefficient (β^p) and (b) volume depolarization ratio (δ^V) during 26 – 31 March, 2015.

Con formato: Espacio Después: 15,5 pto, Interlineado: sencillo

Con formato: Espacio Después: 9,2 pto, Interlineado: sencillo

Con formato: Fuente: 12 pto

Con formato: Fuente: 10,5 pto

Con formato: Fuente: 10,5 pto, Español (España - alfabetización tradicional)

Con formato: Fuente: 10,5 pto

Con formato: Fuente: 10,5 pto, Español (España - alfabetización tradicional)

Con formato: Inglés (Estados Unidos)

Con formato: Espacio Después: 15,5 pto, Interlineado: sencillo

Con formato: Espacio Después: 8 pto, Interlineado: sencillo

Con formato: Fuente: 12 pto

Con formato: Fuente: 10,5 pto

Con formato: Fuente: 10,5 pto, Español (España - alfabetización tradicional)

Con formato: Fuente: 10,5 pto

Con formato: Fuente: 10,5 pto, Español (España - alfabetización tradicional)

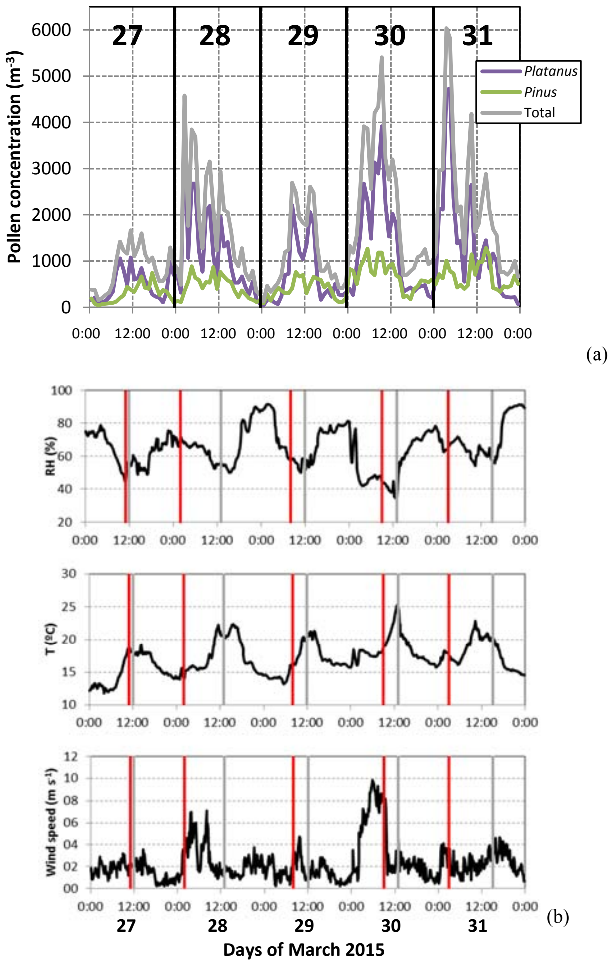

Figure 3. Hourly temporal evolution (a) of the concentration of the two most abundant pollen taxa (*Platanus* and *Pinus*) and (b) of the meteorological data: relative humidity (RH), temperature (T) and wind speed from 00 UT on 27 March until 24 UT on 31 March, 2015. The red and grey vertical lines indicate the time of the maximum pollen concentration and pollen optical depth, respectively, on each day.

Pollen ~~b~~Backscatter coefficient~~s~~ (Mm^{-1} sr^{-1})

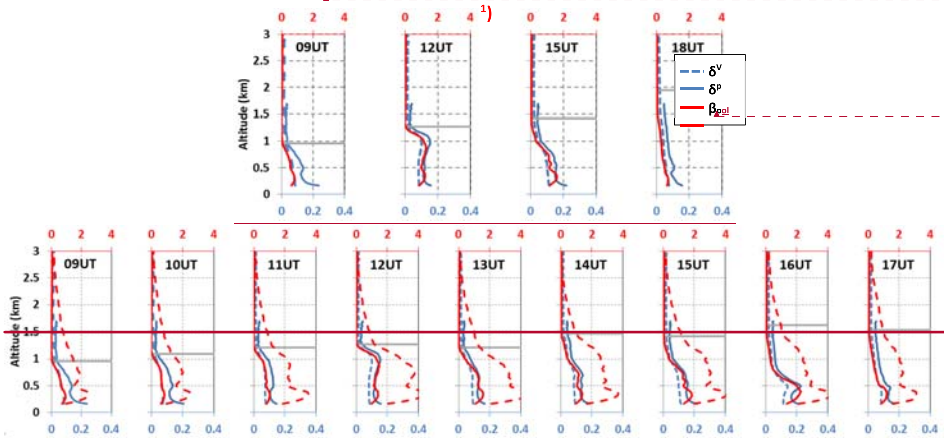

(a)

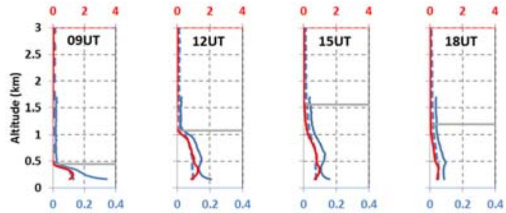

(b)

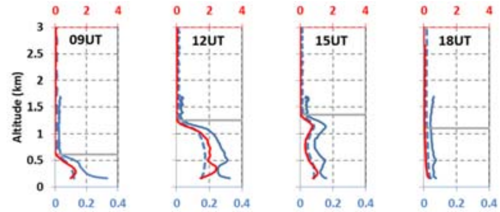

(c)

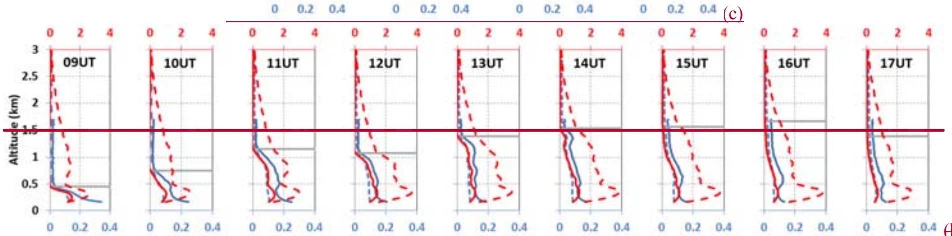

~~(b)~~

Con formato: Inglés (Estados Unidos)

Con formato: Centrado

Con formato: Subíndice

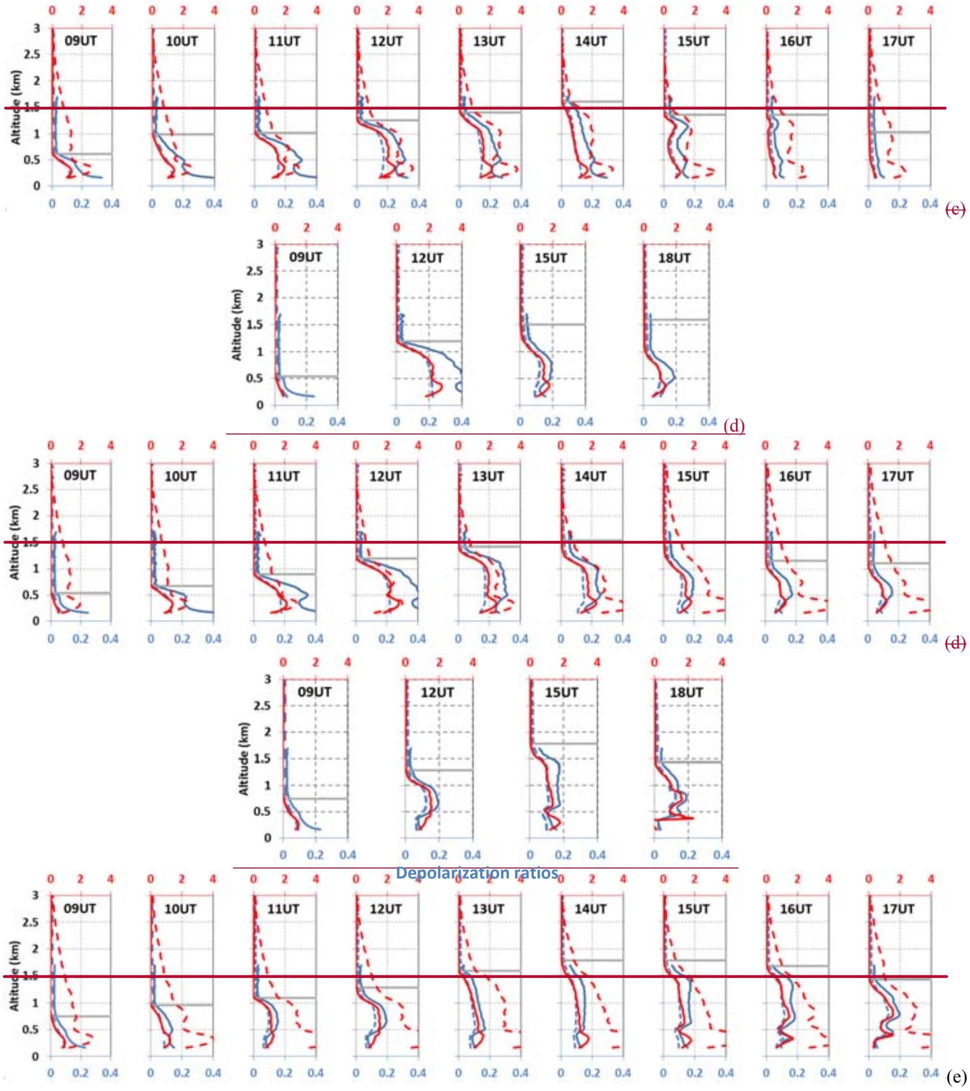

Figure 4. Diurnal time series of the hourly vertical distribution of the ~~particle backscatter coefficient (β^p), the~~ pollen backscatter coefficient (β_{pol}), the volume depolarization ratio (δ^V) and the particle depolarization ratio (δ^p) on (a) 27, (b) 28, (c) 29, (d) 30 and (e) 31 March, 2015. The grey horizontal lines indicate the pollen layer height, h_{pol} .

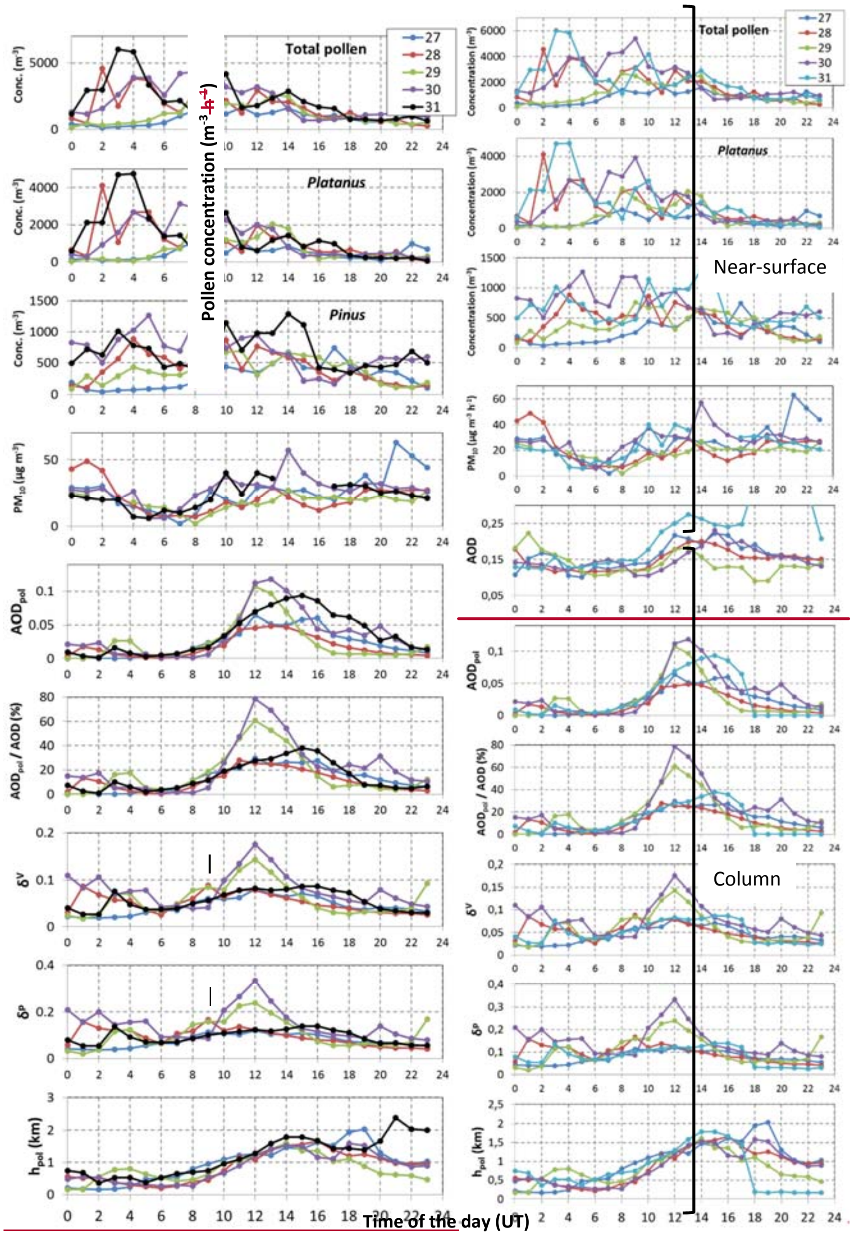

Con formato: Espacio Después: 18 pto

Figure 5. Daily cycle for all five days of the pollination event of the total pollen, the *Platanus* and the *Pinus* concentration, PM_{10}, ~~AOD,~~ AOD_{pol}, AOD_{pol} /AOD, $\overline{\delta^V}$ ~~δ^V, δ^p~~ $\overline{\delta^p}$ and h_{pol} ~~and h_{pol}~~ (see legend in the top plot).

Código de campo cambiado

Código de campo cambiado

Código de campo cambiado

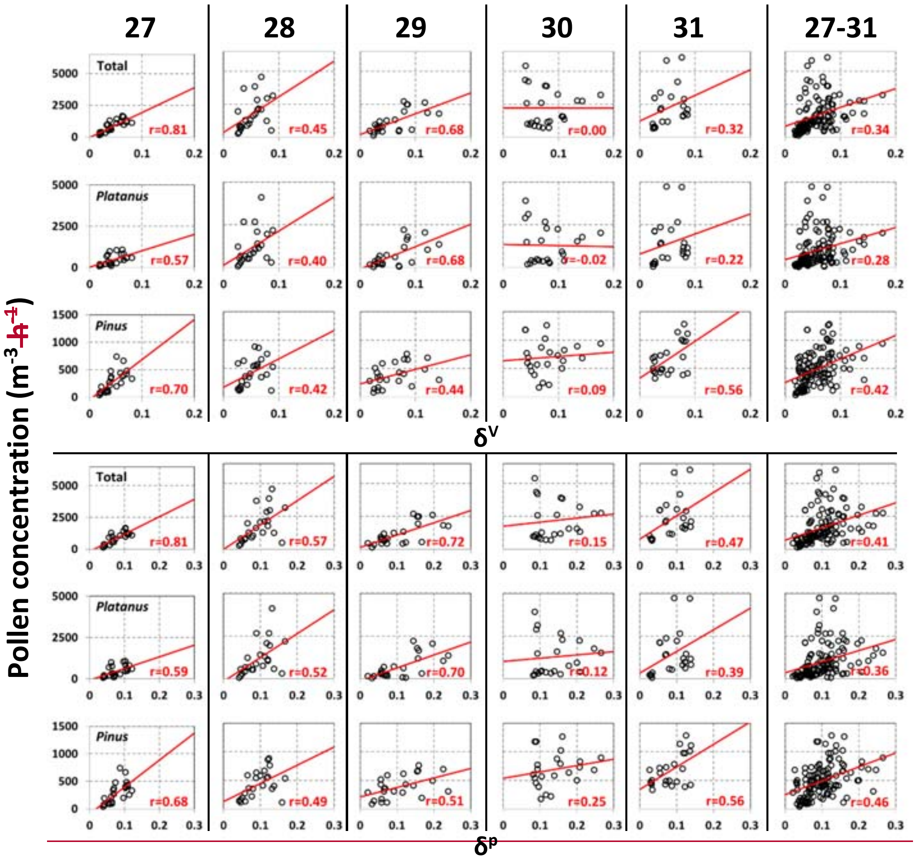
27
28
29
30
31
27-31
Total
Platanus
Pinus
Pollen concentration (m-3 h-1)
r=0.81
r=0.45
r=0.68
r=0.00
r=0.32
r=0.34
r=0.57
r=0.40
r=0.68
r=-0.02
r=0.22
r=0.28
r=0.70
r=0.42
r=0.44
r=0.09
r=0.56
r=0.42
δV
r=0.81
r=0.57
r=0.72
r=0.15
r=0.47
r=0.41
r=0.59
r=0.52
r=0.70
r=0.12
r=0.39
r=0.36
r=0.68
r=0.49
r=0.51
r=0.25
r=0.56
r=0.46
δP

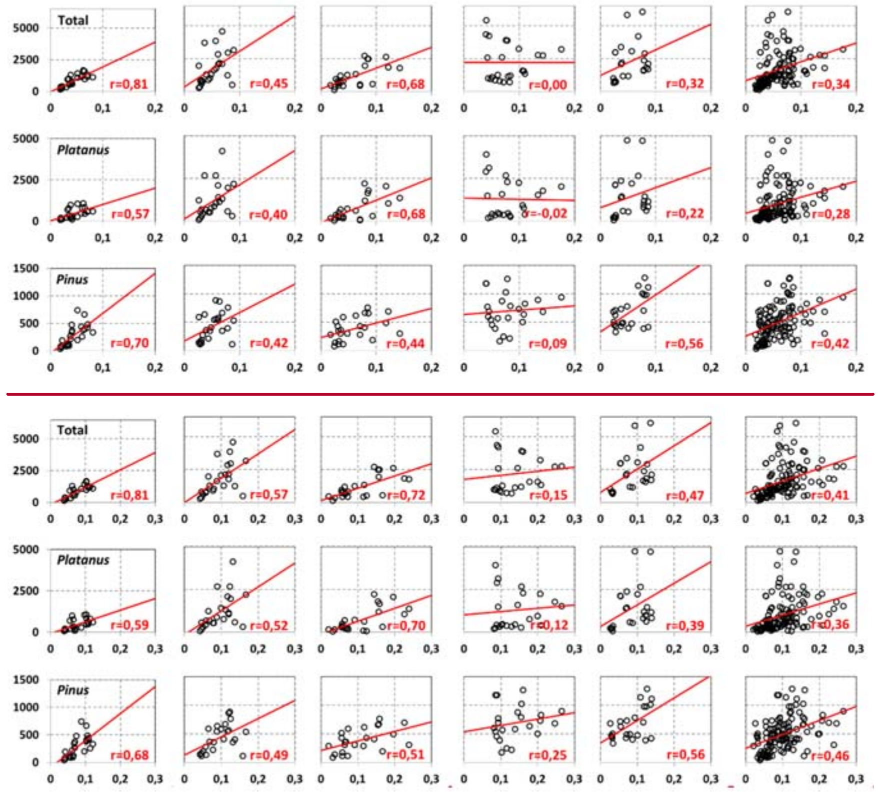

Figure 6. Scatter plot of the pollen concentration (total, *Platanus* and *Pinus*) vs. the volume ($\overline{\delta^V}$) and the particle ($\overline{\delta^p}$) depolarization ratio integrated in the pollen plume for all five days of the pollination event. The linear regression line is in red and the correlation coefficient, *r*, is reported.

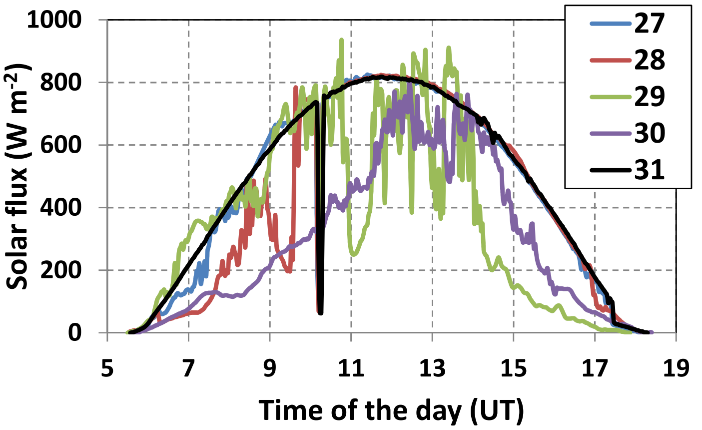

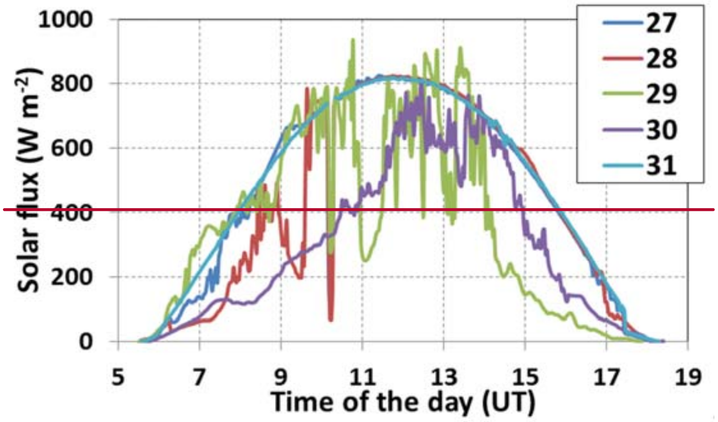

Figure 7. Diurnal cycle for all five days of the pollination event of the total downward solar flux measured in the range 0.3 – 2.8 µm at ground level close to the lidar station.

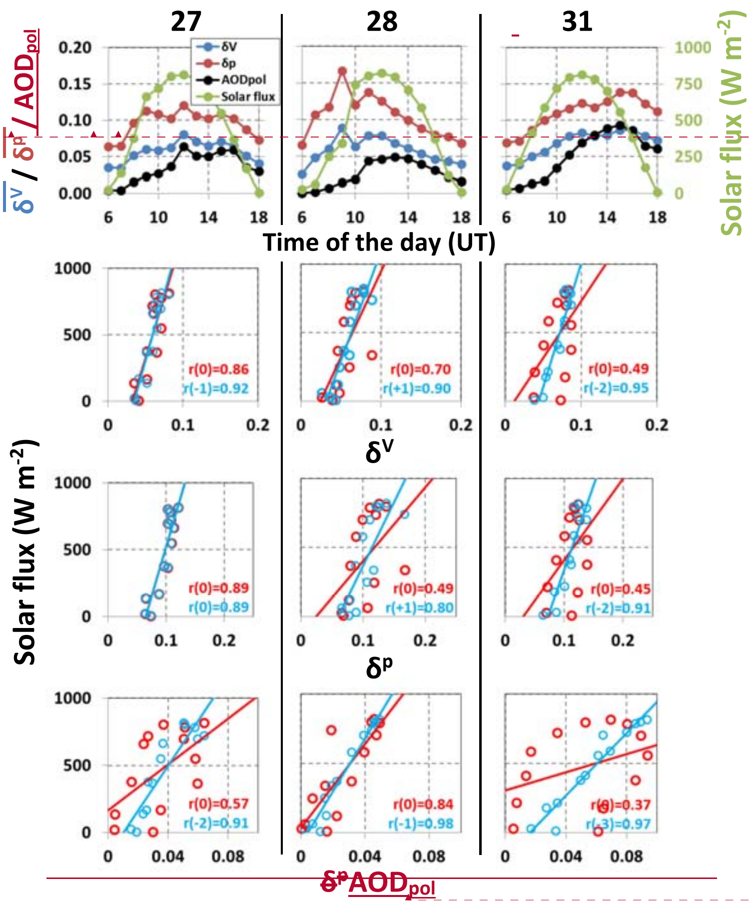

Con formato: Fuente: 15 pto, Color de fuente: Énfasis 1

Con formato: Fuente: 15 pto

Con formato: Fuente: 15 pto, Color de fuente: Énfasis 2

Con formato: Fuente: 15 pto

Con formato: Fuente: 15 pto, Subíndice

Con formato: Fuente: 15 pto

Con formato: Subíndice

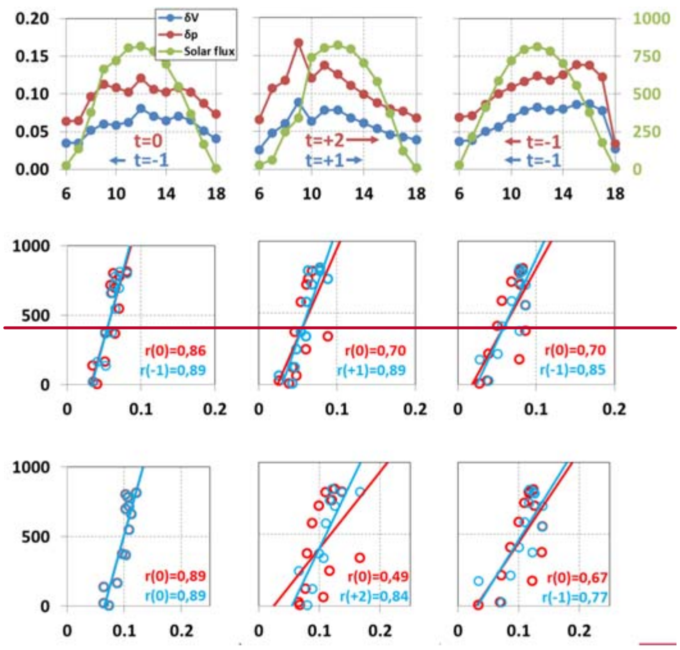

Figure 8. (top) Diurnal evolution of $\overline{\delta^V}$, $\overline{\delta^p}$ ~~and~~ AOD$_{pol}$ and solar fluxes on 27, 28 and 31 March between 06 and 18 UT; (cente/top~~r~~) scatter plot of the solar flux vs. $\overline{\delta^V}$; (center/bottom) scatter plot of the solar flux vs. $\overline{\delta^p}$ ~~.~~; (bottom) scatter plot of the solar flux vs. AOD$_{pol}$. In each scatter plot, straight lines are linear regression lines; the red color corresponds to *t*=0; the blue color corresponds to *t*=*t$_{opt}$*. The values of *r*(*t*) are reported in each scatter plot.

Con formato: Subíndice

Con formato: Subíndice

0 – 24 UT

	Units	27	28	29	30	31	27-31
Conc. total	m^{-3}	865	1770	1141	2201	2237	1643
Conc. *Platanus*	m^{-3}	474	1181	690	1301	1384	1006
Conc. *Pinus*	m^{-3}	286	433	387	700	668	495
PM_{10}	µg m^{-3}	25.7	21.4	18.2	27.5	22.8	23.2
AOD		0.16	0.15	0.14	0.15	0.24	0.17
AOD_{pol}		0.02	0.02	0.02	0.04	0.0~~3~~4	0.03
AOD_{pol} / AOD	%	12	11	17	23	1~~2~~4	15
$\overline{\delta^v}$		0.04	0.05	0.06	0.08	0.0~~5~~6	0.06
$\overline{\delta^p}$		0.08	0.10	0.11	0.15	0.0~~8~~9	0.10
h_{pol}	km	0.98	0.87	0.81	0.85	~~0.77~~1.18	0.~~86~~94

9 – 17 UT

	Units	27	28	29	30	31	27-31
Conc. Total	m^{-3}	1251	1909	1779	2338	2364	1928
Conc. *Platanus*	m^{-3}	640	1169	1133	1489	1321	1150
Conc. *Pinus*	m^{-3}	458	547	580	635	832	610
PM_{10}	µg m^{-3}	23.9	17.6	18.6	34.8	31.7	25.3
AOD		0.19	0.17	0.14	0.16	0.23	0.18
AOD_{pol}		0.05	0.03	0.05	0.06	0.07	0.05
AOD_{pol} / AOD	%	23	20	34	40	27	29
$\overline{\delta^v}$		0.07	0.06	0.09	0.10	0.08	0.08
$\overline{\delta^p}$		0.11	0.11	0.15	0.18	0.12	0.14
h_{pol}	km	1.31	1.22	1.18	1.11	1.37	1.24

Table 1. Mean parameters during the pollination event calculated over the periods of 0 – 24 and 9 – 17 UT.

Tabla con formato

0 – 24 UT

	27	28	29	30	31	27-31
PM_{10}	0.01	-0.24	-0.50	-0.37	-0.28	-0.18
AOD	0.41	-0.34	-0.09	-0.61	-0.53	-0.18
AOD_{pol}	0.65	0.03	0.64	-0.25	0.~~05~~23	0.~~12~~07
AOD_{pol} / AOD	0.74	0.06	0.68	-0.16	0.05~~0.12~~ -	0.1~~5~~3
$\overline{\delta^v}$	**0.81**	0.45	0.68	0.00	0.~~32~~14	0.343
$\overline{\delta^p}$	**0.81**	**0.57**	**0.72**	**0.15**	**0.~~47~~26**	**0.4~~1~~0**
h_{pol}	0.54	-0.42	0.46	-0.59	-0.~~12~~59	- 0.~~11~~22

9 – 17 UT

	27	28	29	30	31	27-31
PM_{10}	-0.22	0.19	-0.28	-0.32	**0.22**	0.18
AOD	-0.23	-0.24	0.41	-0.88	-0.58	-0.13
AOD_{pol}	-0.19	-0.05	0.55	-0.26	-0.50	0.12
AOD_{pol} / AOD	-0.09	-0.03	0.58	-0.03	-0.46	0.18
$\overline{\delta^v}$	-0.05	**0.77**	0.65	0.07	-0.63	0.33
$\overline{\delta^p}$	-0.08	0.72	**0.68**	**0.23**	-0.56	**0.37**
h_{pol}	-0.22	-0.68	-0.05	-0.69	-0.41	-0.35

Table 2. Correlation coefficients of total pollen during the pollination event calculated over the periods of 0 – 24 and 9 – 17 UT. Bold numbers indicate for each day the parameter with the highest positive correlation coefficient. Numbers in red indicate for each parameter the day with the highest positive correlation coefficient.

Tabla con formato

Tabla con formato

0 – 24 UT

	27	28	29	30	31	27-31
PM_{10}	-0.03	-0.10	-0.49	-0.33	-0.37	-0.19
AOD	0.14	-0.34	0.00	-0.55	-0.53	-0.22
AOD_{pol}	0.36	-0.03	0.63	-0.23	-0.0732	0.051
AOD_{pol} / AOD	0.44	-0.01	0.65	-0.15	- 0.150.01	0.097
$\overline{\delta^V}$	0.57	0.40	0.68	-0.02	0.2206	0.286
$\overline{\delta^p}$	**0.59**	**0.52**	**0.70**	**0.12**	**0.319**	**0.364**
h_{pol}	0.22	-0.44	0.36	-0.55	-0.0264	- 0.1629

9 – 17 UT

PM_{10}	-0.08	0.18	-0.23	-0.35	-0.03	0.04
AOD	-0.23	-0.19	0.57	-0.85	-0.76	-0.33
AOD_{pol}	-0.14	-0.04	0.66	-0.32	-0.67	-0.01
AOD_{pol} / AOD	-0.03	-0.04	0.66	-0.11	-0.62	0.12
$\overline{\delta^V}$	0.18	**0.74**	**0.70**	-0.02	-0.78	0.29
$\overline{\delta^p}$	**0.30**	0.68	**0.70**	**0.14**	-0.65	**0.36**
h_{pol}	-0.43	-0.63	0.04	-0.72	-0.56	-0.48

Table 3. Idem as Table 2Table 2 for *Platanus*.

0 – 24 UT

	27	28	29	30	31	27-31
PM_{10}	0.12	-0.51	-0.22	-0.39	0.32	-0.06
AOD	0.62	-0.15	-0.26	-0.75	-0.19	0.03
AOD_{pol}	0.76	0.27	0.43	-0.29	0.~~54~~36	0.29
AOD_{pol} / AOD	**0.80**	0.27	0.55	-0.17	**0.~~54~~46**	0.29
$\overline{\delta^{v}}$	0.70	0.42	0.44	0.09	0.~~56~~44	0.42
$\overline{\delta^{p}}$	0.68	**0.49**	0.51	**0.25**	0.~~56~~45	**0.4~~6~~7**
h_{pol}	0.76	-0.19	**0.63**	-0.65	0.~~5~~02	0.0~~9~~8

9 – 17 UT

PM_{10}	-0.16	**0.49**	-0.21	-0.14	**0.81**	**0.26**
AOD	0.13	-0.04	-0.61	-0.86	0.27	0.02
AOD_{pol}	0.00	0.14	-0.43	-0.04	0.32	0.15
AOD_{pol} / AOD	-0.03	0.17	-0.29	0.21	0.31	0.14
$\overline{\delta^{v}}$	-0.45	0.45	-0.18	0.30	0.20	0.19
$\overline{\delta^{p}}$	-0.79	0.38	-0.07	**0.44**	0.10	0.22
h_{pol}	**0.59**	-0.42	-0.33	-0.54	0.29	-0.08

Table 4. Idem as Table 2~~Table 2~~ for *Pinus*.

Con formato: Fuente: Negrita

Con formato: Fuente: Sin Negrita

Con formato: Fuente: Sin Negrita

Página 12: [1] Con formato	msicard	12/05/2016 15:18:00

Fuente: (Predeterminada) Times New Roman, 10 pto

Página 12: [2] Con formato	msicard	12/05/2016 15:18:00

Fuente: (Predeterminada) Times New Roman, 10 pto

Página 12: [3] Con formato	msicard	12/05/2016 15:18:00

Fuente: (Predeterminada) Times New Roman, 10 pto

Página 12: [4] Con formato	msicard	12/05/2016 15:18:00

Fuente: (Predeterminada) Times New Roman, 10 pto

Página 12: [5] Con formato	msicard	12/05/2016 15:18:00

Fuente: (Predeterminada) Times New Roman, 10 pto

Página 12: [6] Con formato	msicard	12/05/2016 15:18:00

Fuente: (Predeterminada) Times New Roman, 10 pto

Página 12: [7] Con formato	msicard	12/05/2016 15:18:00

Fuente: (Predeterminada) Times New Roman, 10 pto

Página 12: [8] Con formato	msicard	12/05/2016 15:18:00

Fuente: (Predeterminada) Times New Roman, 10 pto

Página 12: [9] Con formato	msicard	12/05/2016 15:18:00

Fuente: (Predeterminada) Times New Roman, 10 pto

Página 12: [10] Con formato	msicard	12/05/2016 15:18:00

Fuente: (Predeterminada) Times New Roman, 10 pto